Billion particle simulations of cosmic dark matter and phase transitions

A) N-body simulations of galactic dark matter

B) Molecular dynamics simulations of phase transitions

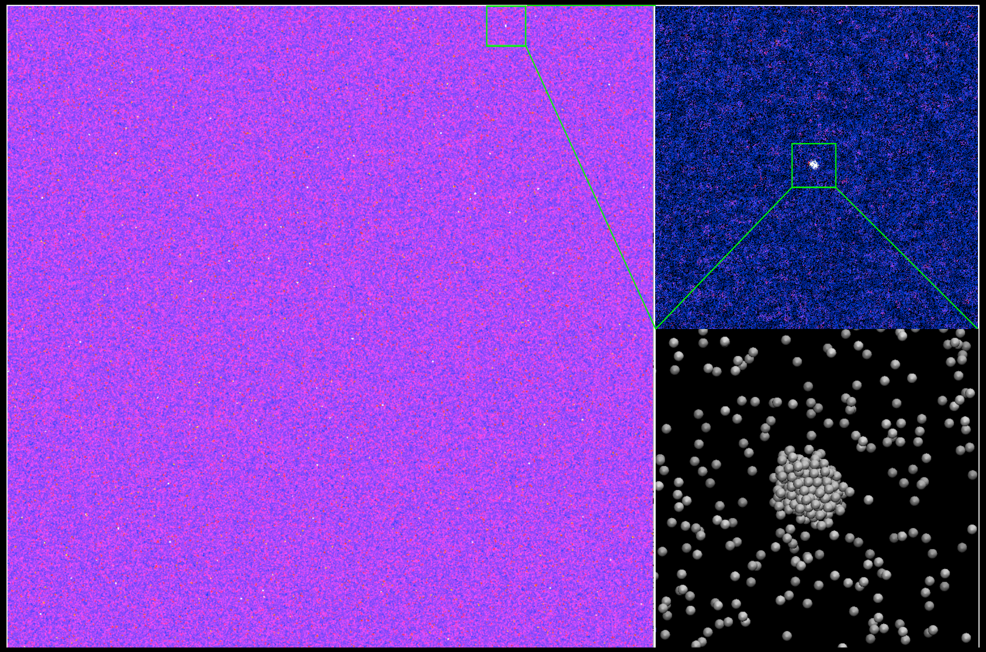

Jürg Diemand, Computational Science / Theoretical Physics, University of Zurich

Monday, 18th of November, 2013, RIKEN AICS, Kobe

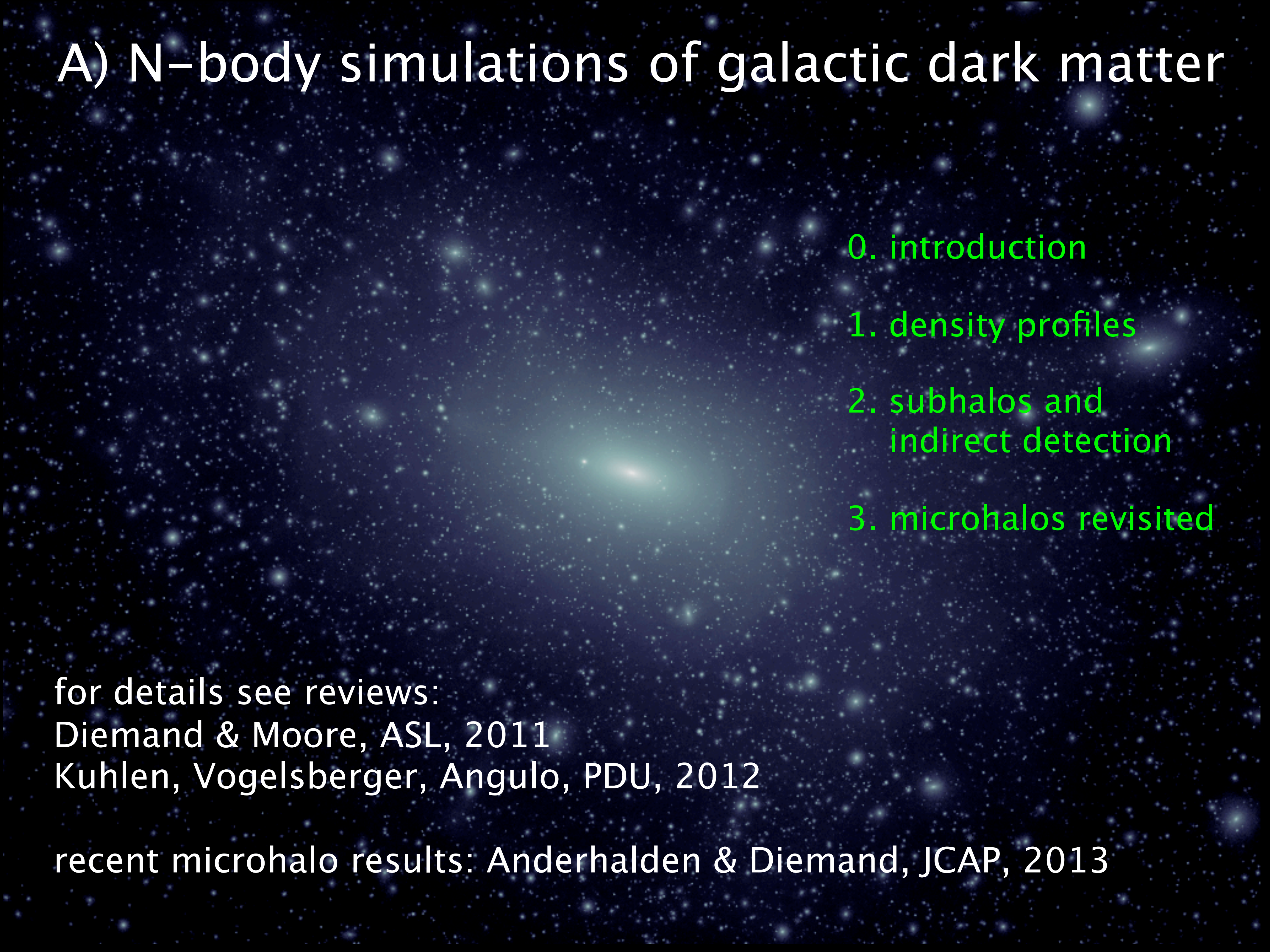
A) N-body simulations of galactic dark matter
0. introduction
1. density profiles
2. subhalos and indirect detection
3. microhalos revisited
for details see reviews:
Diemand & Moore, ASL, 2011
Kuhlen, Vogelsberger, Angulo, PDU, 2012
recent microhalo results: Anderhalden & Diemand, JCAP, 2013

Dark matter dominates structure formation

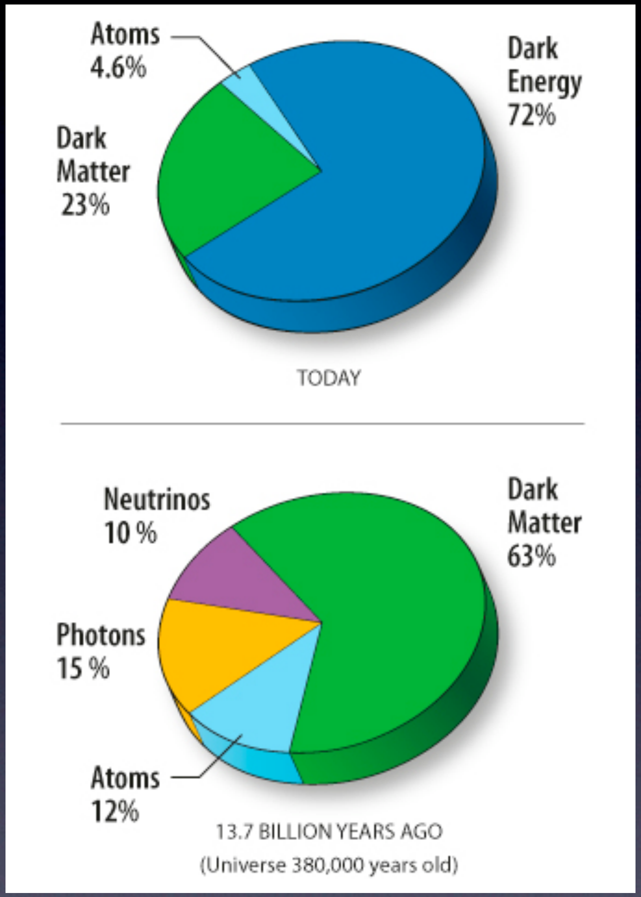

NASA / WMAP Science Team

collision-less simulations
(pure N-body, dark matter only)
treat all matter like dark matter

no free parameters
high resolution, good scaling

good approximation for dwarf galaxy halos and for smaller, dark halos and subhalos

not accurate near centers of galaxies

accurate solution of idealized problem

one main motivation:
DM annihilation signal ~ density^2
i.e. structures on all scales increase the signal

Simulating structure formation

N-body models approximating CDM halos (about 1995 to 2000)

log density

N_halo from about 10k to a million

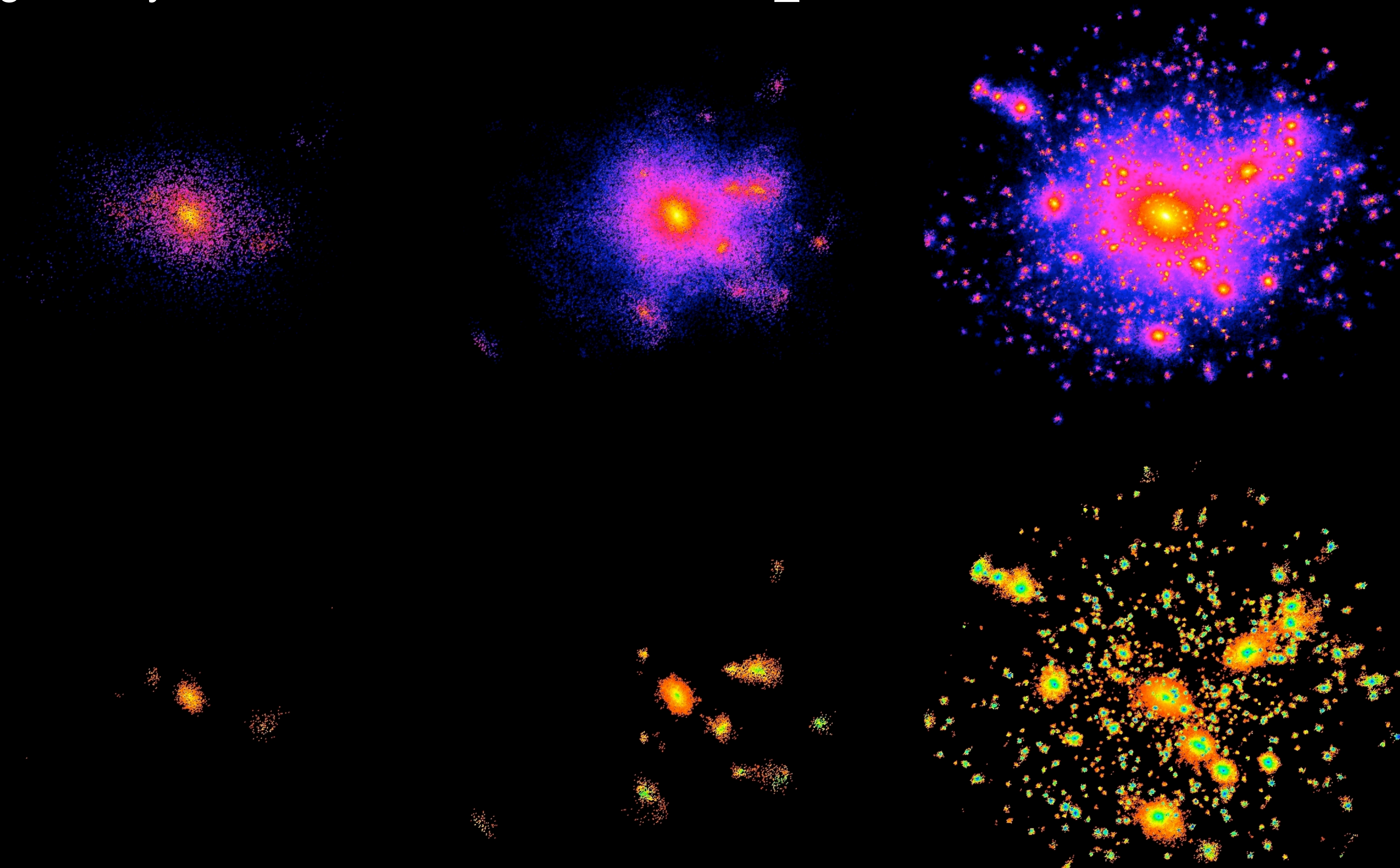

log phase space density

from Ben Moore : www.nbody.net

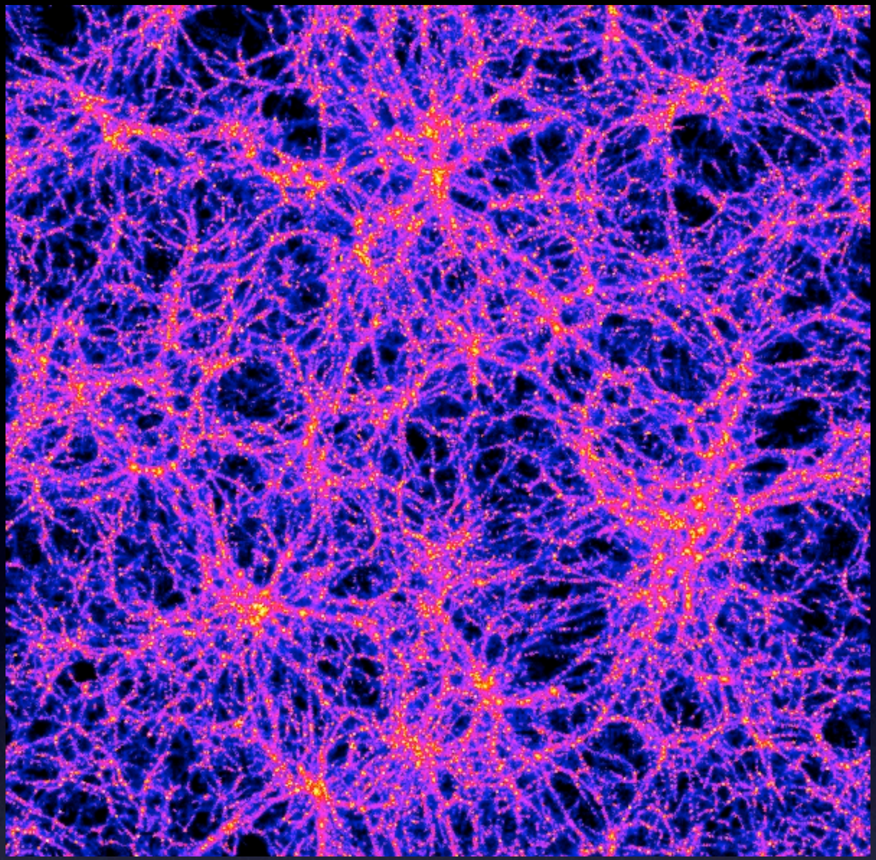

uniform resolution, periodic cubes

- good statistics, lower resolution
- large scale structure
- fair sample of halos and environments

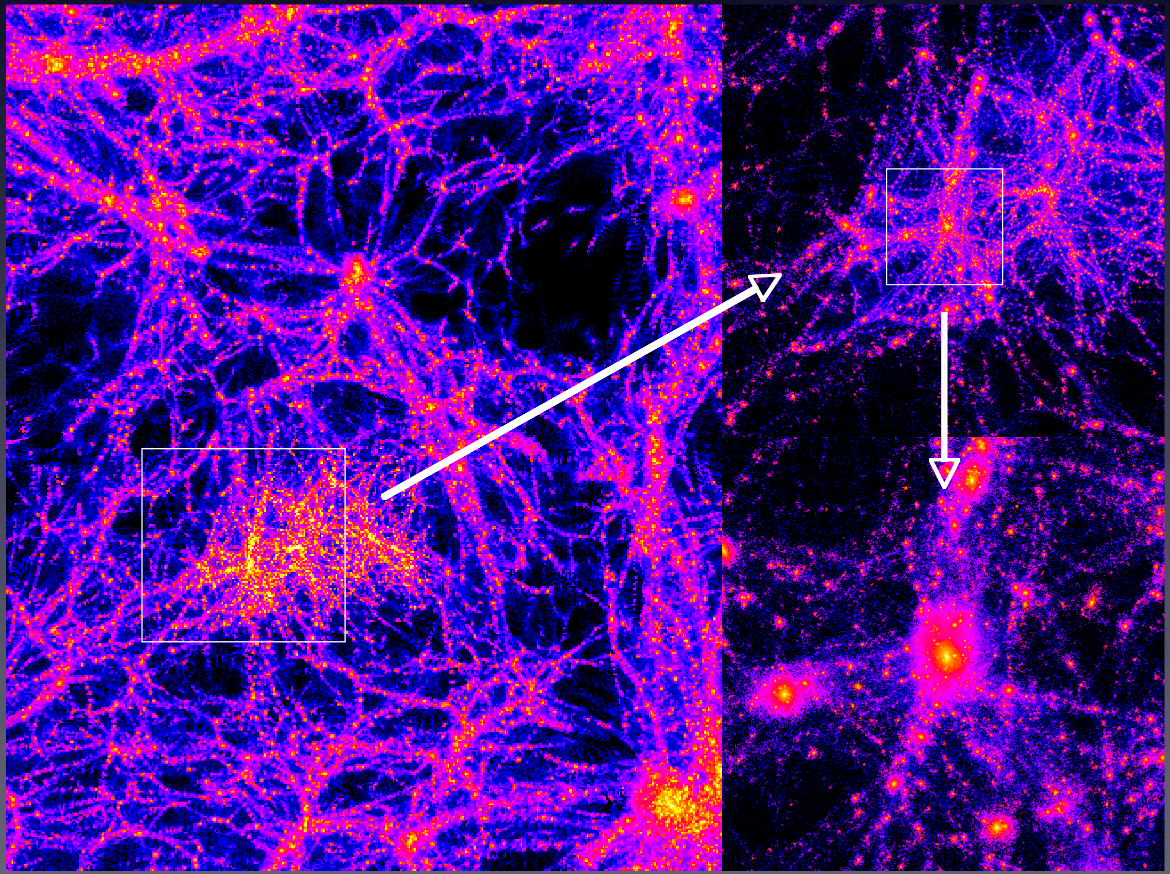

refined, re-simulations of individual halos

- low statistics, high resolution
- selection effects?
  see e.g. Ishiyama et al 2008

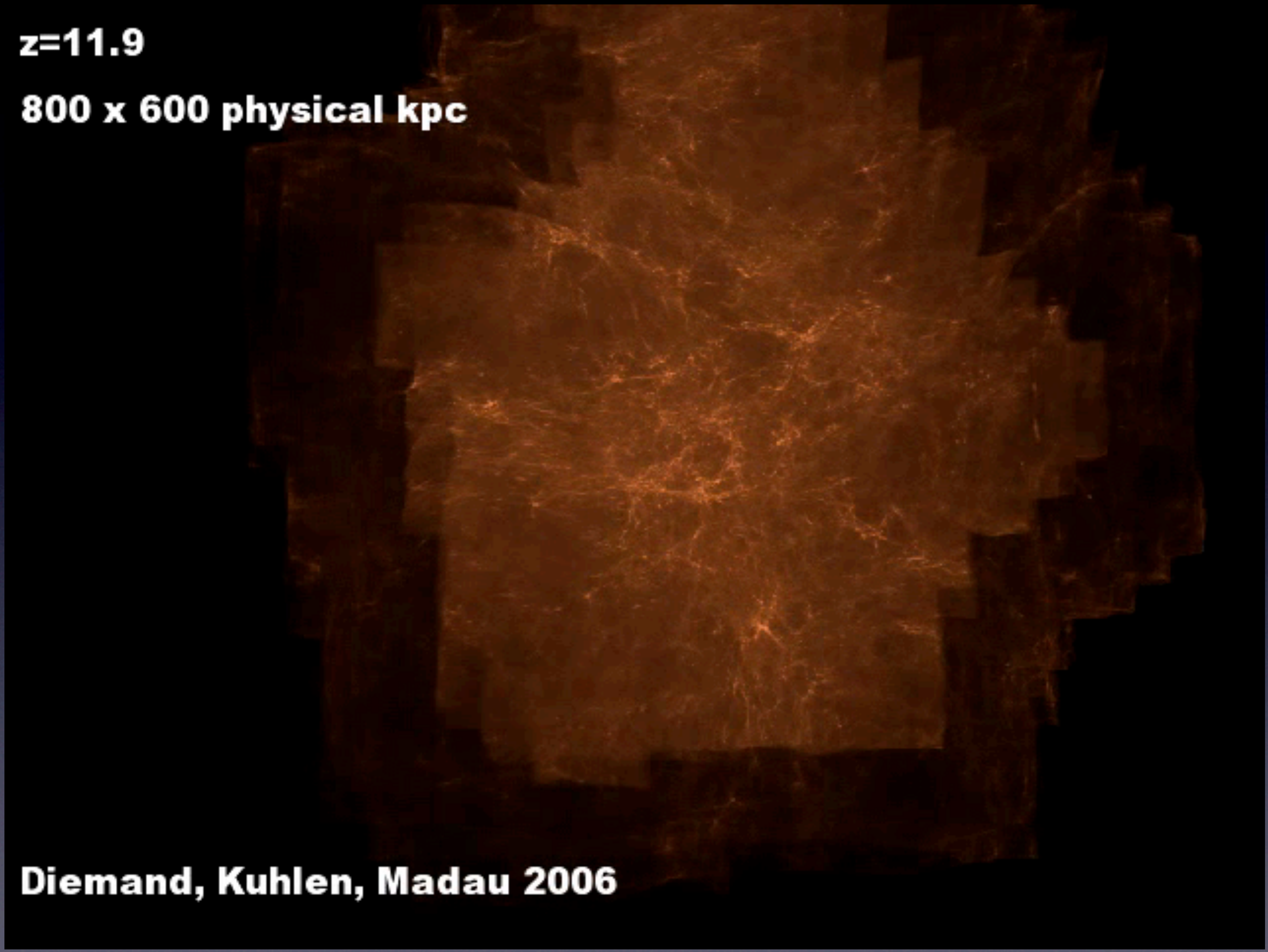
z=11.9
800 x 600 physical kpc
Diemand, Kuhlen, Madau 2006

via lactea II at redshift zero

www.physik.uzh.ch/~diemand/vl

the via lactea project

high resolution Milky Way dark matter halos simulated on NASA's Columbia and ORNL's Jaguar supercomputers

VL-2 movies

This movie rotates and zooms into the via lactea-2 halo at z=0 (today). The colors show the local dark matter densities.

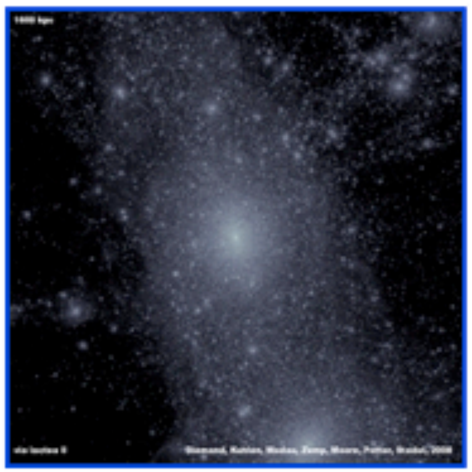

- slow rotation (larger files) : high quality (174 MB) medium (43 MB) low (18 MB)
- fast rotation (smaller files) : high quality (87 MB) medium (24 MB) low (12 MB)

VL-1 movies

These animations show the projected dark matter density-square maps of the simulated Milky Way-size halo via lactea-1. The logarithmic color scale covers the same 20 decades in projected density-square in physical units in each frame. All movies are encoded in MPEG format and some are available in different quality versions.

the formation of the via lactea halo

- entire formation history (z=12 to 0): high quality (218 MB)
  smaller frames, quality: high(55 MB) medium(11 MB) low(4.7 MB)
- entire formation history, plus rotation and zoom at z=0:

What is a (sub)halo? Operational definitions

mass profiles around peaks in (phase-space) density

$V_{circ}^2 = GM(<r)/r$
has a well defined peak:
V_{max} at r_{Vmax}

no clear outer boundary: "virial" radius is a simple, but arbitrary scale
Anderhalden&JD 2011

halos with the virial radius of another are called subhalos

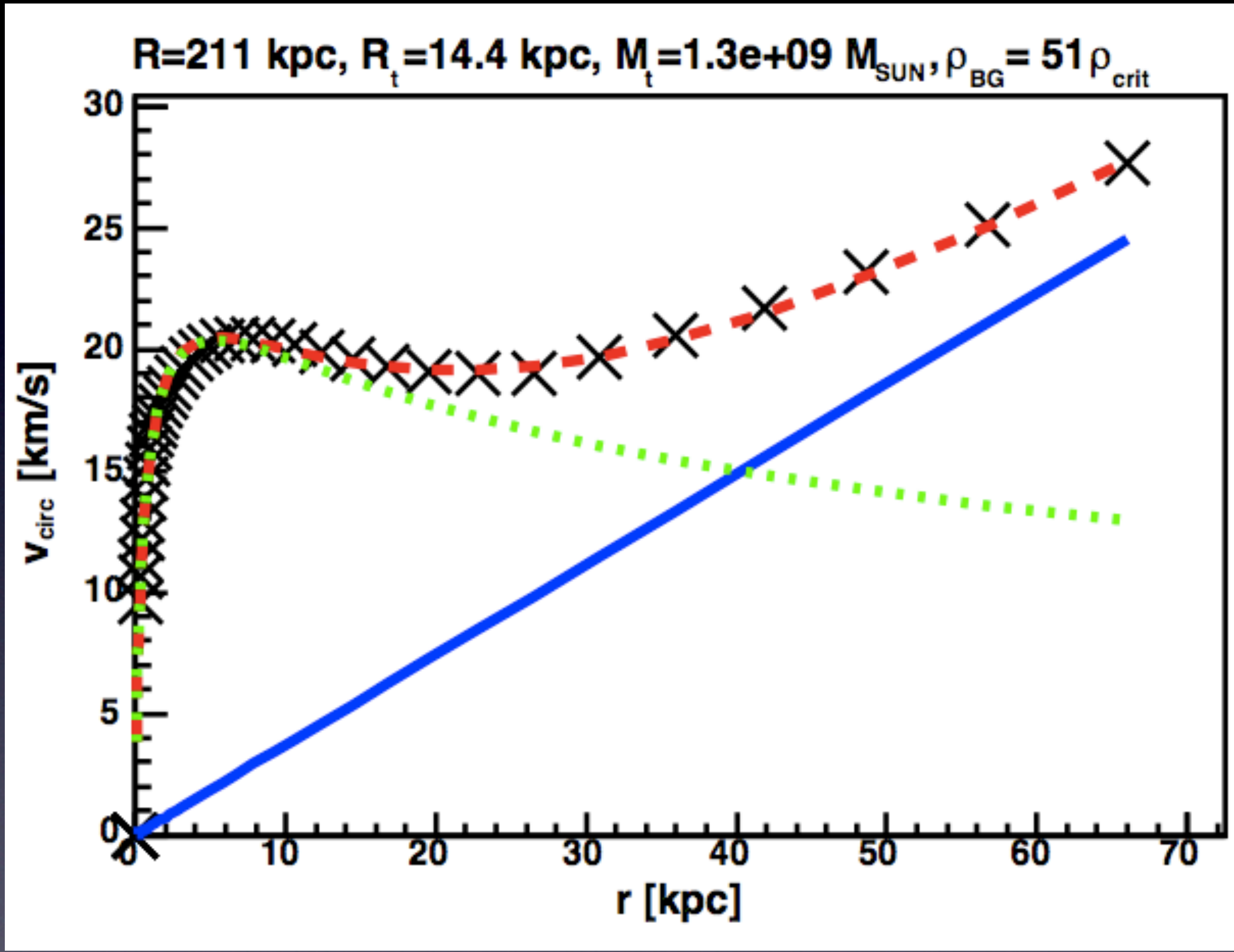

(sub)halo concentrations:
$c_V = rho(<r_{Vmax}) / rho_{crit,z=0}$
$c_{NWF} = r_{vir} / r_s$, $r_s = r_{Vmax} / 2.16$

1. density profiles

main halo density profile

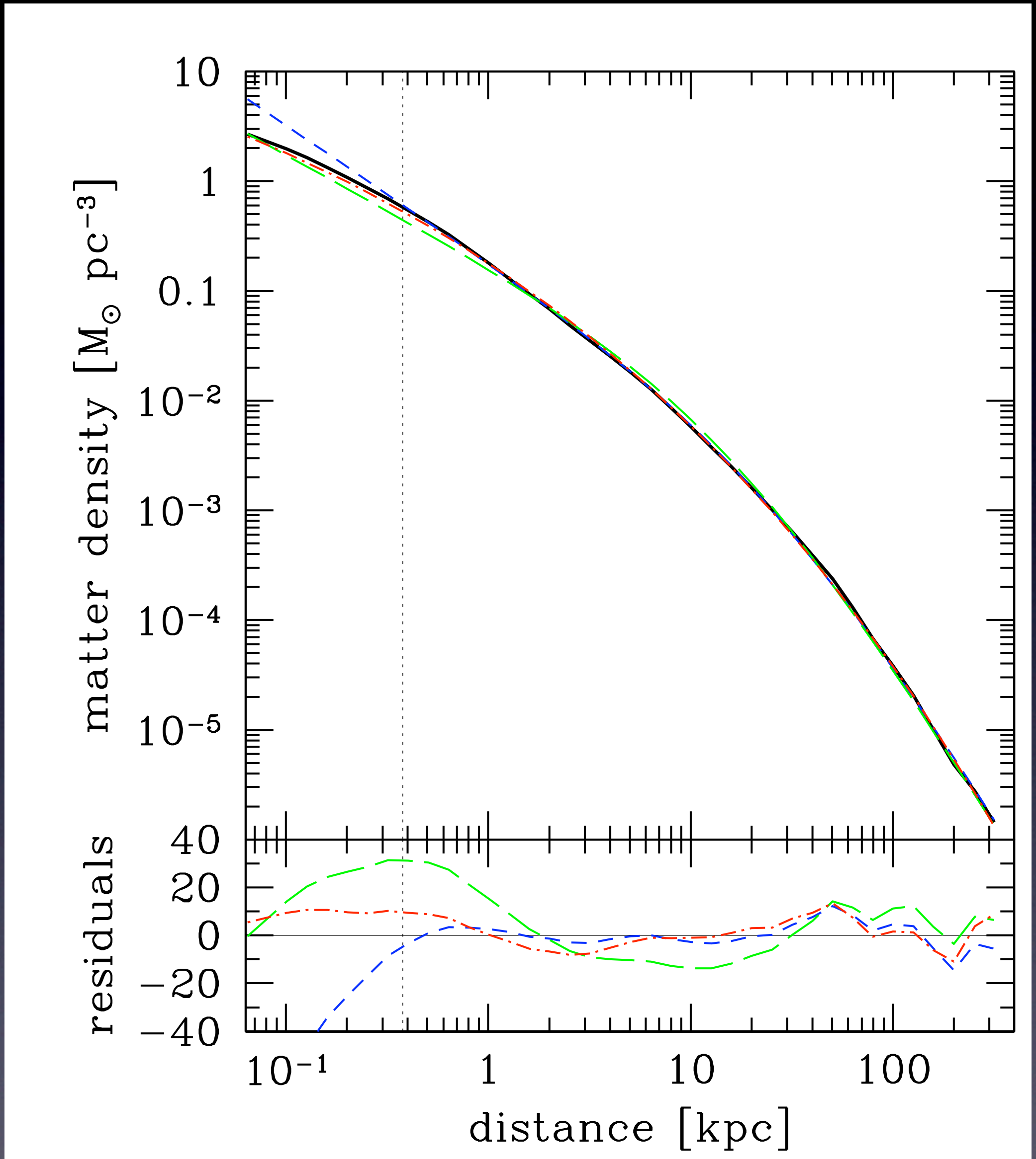

NFW
Einasto
$r^{-1.24}$ inner profile

JD et al. Nature 2008

inner region is denser than NFW: Einasto and $r^{-1.24}$ fit well down to 400 pc.
probably shallower than $r^{-1.24}$ on very small scales (scatter / convergence?).

main halo density profile

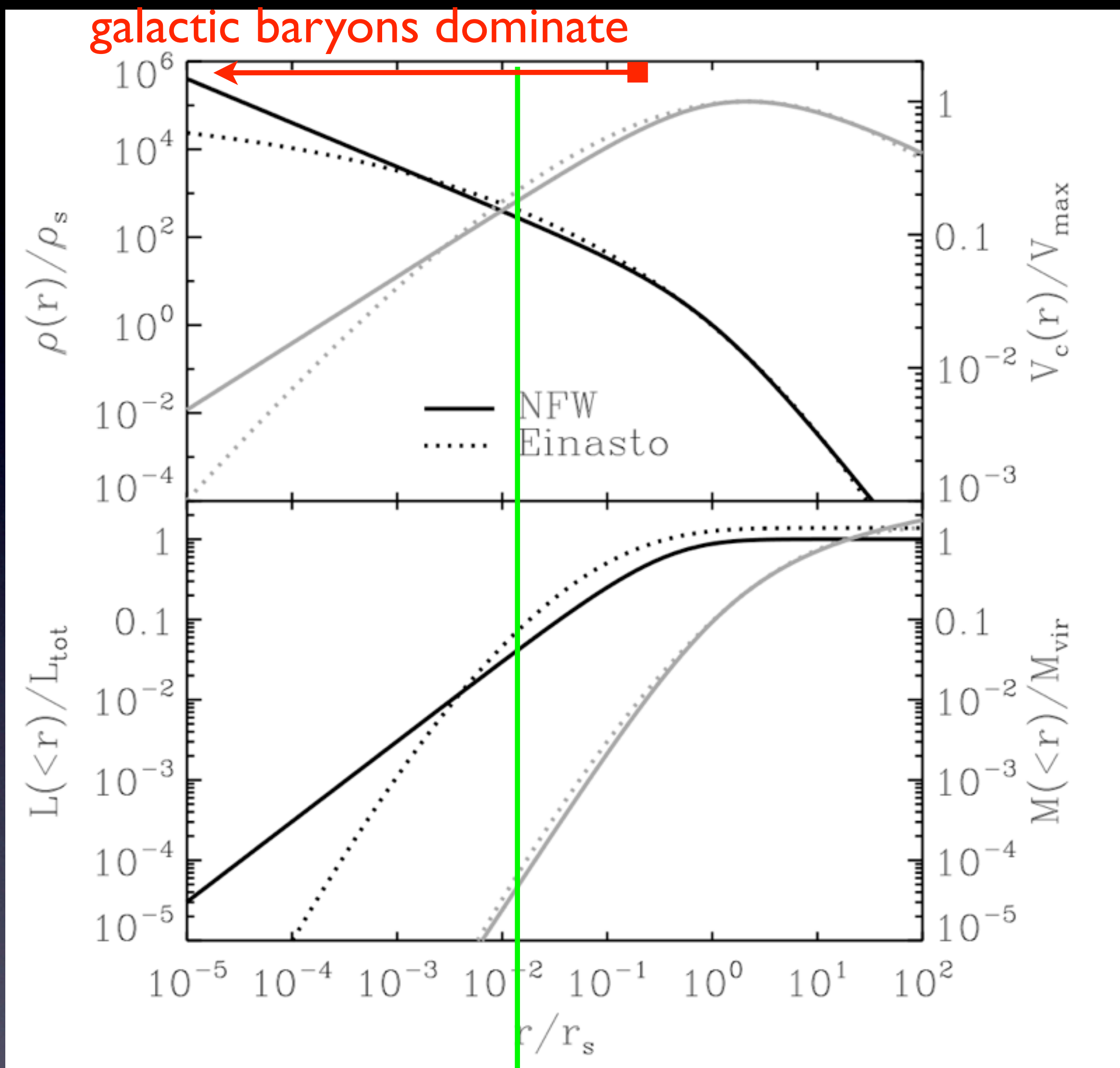

Kuhlen, AdAst 2010

comparison of NFW and Einasto (alpha=0.17) profiles

normalized at Vmax and rVmax

$L_{Einasto} = 1.41\ L_{NFW}$

well resolved region in pure dark matter simulations contains > 99 percent of the annihilation luminosity L (Einasto and $r^{-1.24}$ inner profile are very similar here)

2. subhalos and indirect detection

subhalo and sub-subhalo abundance

$$L \propto \rho_s^2 r_s^3 \propto V_{\rm max}^4 / r_{\rm Vmax} \propto V_{\rm max}^3 \sqrt{c_V}$$

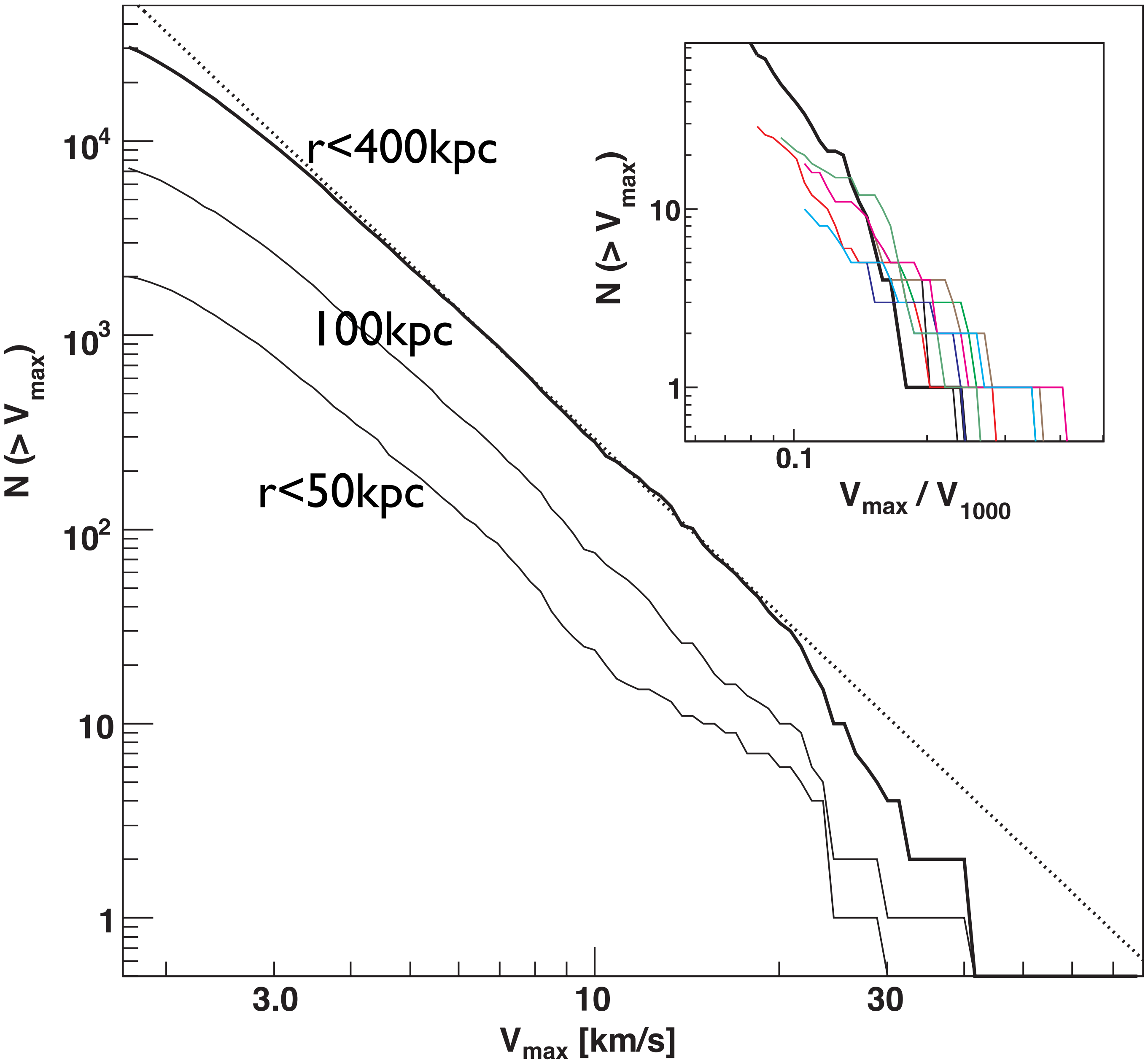

velocity function
N(>V) ~ V^{-3}

annihilation signal has not converged yet in simulations

both for main halos and for subhalos

mass functions
N(>M) ~ $M^{-(0.9 \text{ to } 1.0)}$
give same conclusion

JD et al. Nature 2008

sub-subhalos in all well resolved subhalos

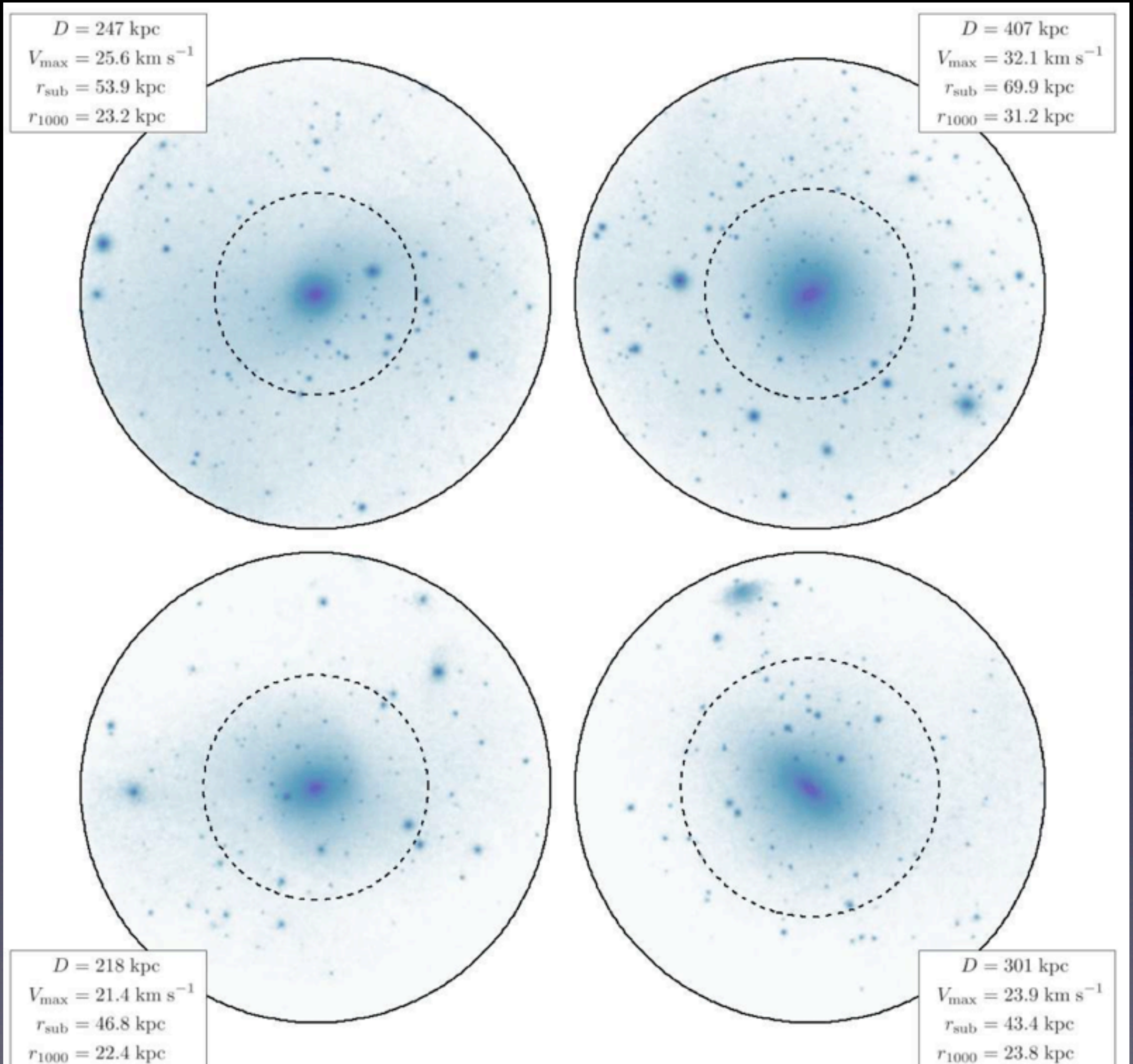

Kuhlen, JD, Madau ApJ 2008

inner subhalo density profiles resemble main halo profiles

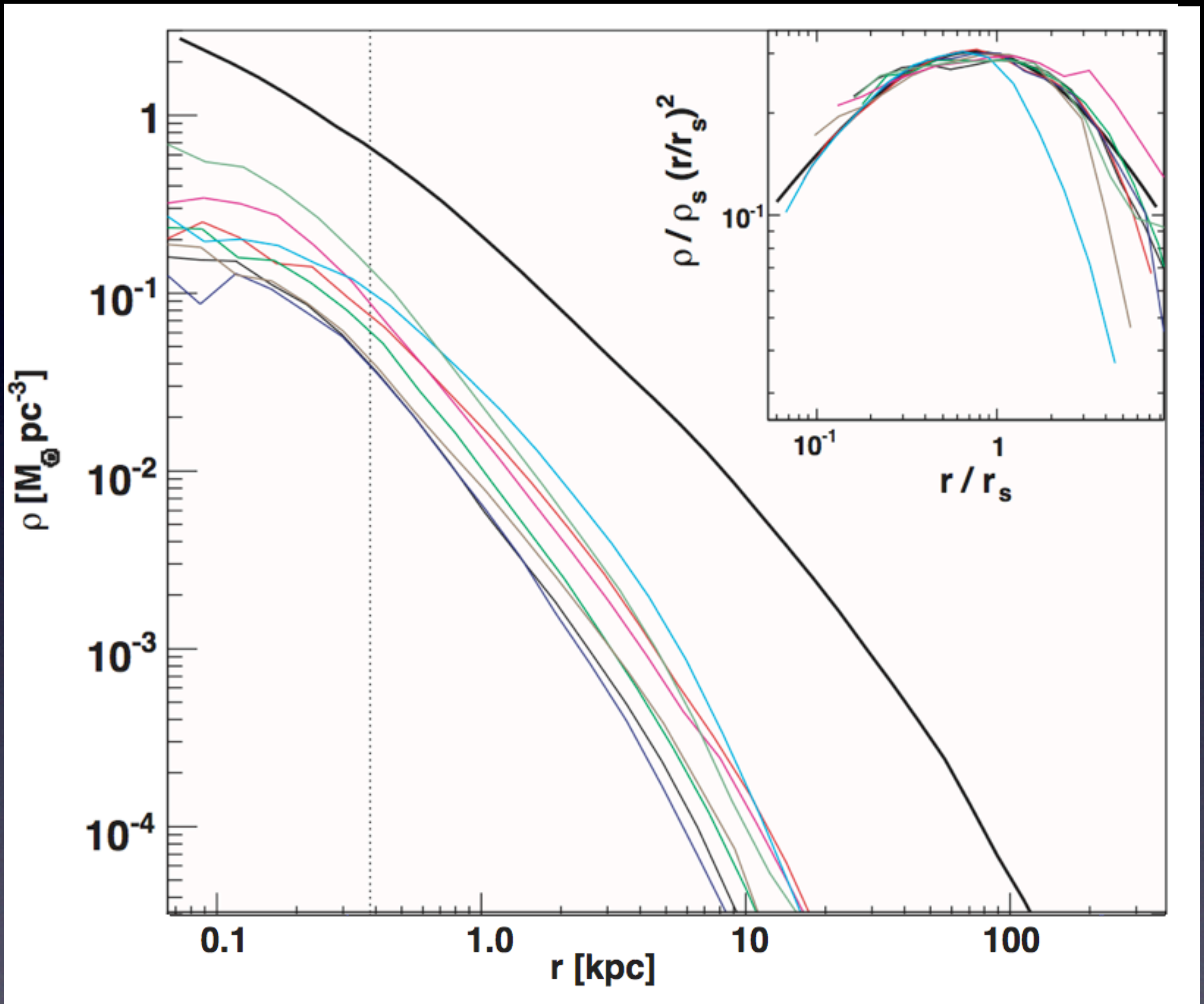

JD et al. Nature 2008

normalized profiles

overlap in inner regions

subhalos fall off steeper in the outer parts

where are the subhalos?

spatial distribution **depends strongly** on how the subhalo sample is **selected**

mass selected subhalos
are found at larger radii than
the dark matter
this 'anti-bias' is smaller in V_{max} selected samples

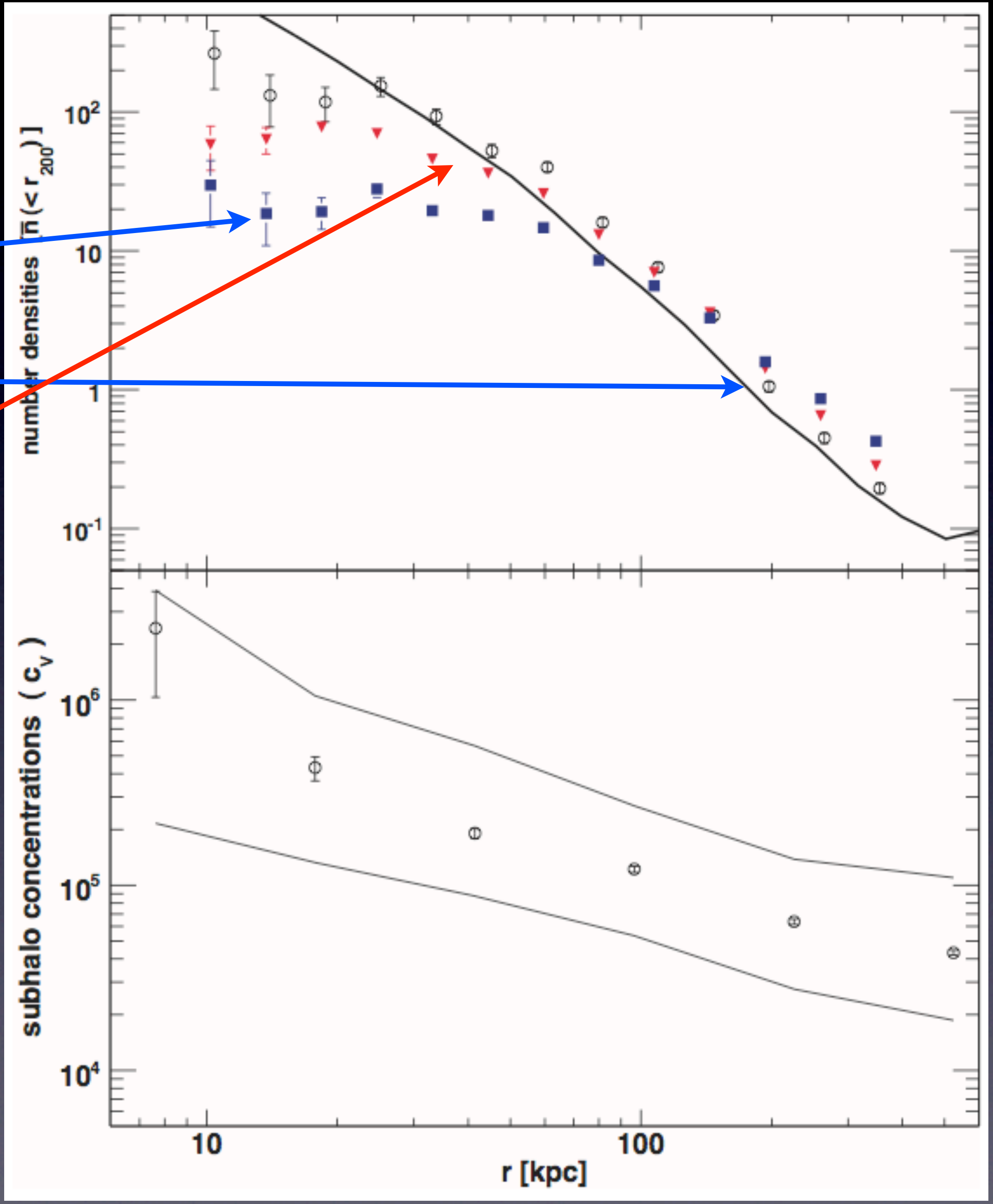

JD&Moore, ASL 2011

no bias when size at accretion is used
Faltenbacher & JD 2005

denser parts survive, subhalo concentrations increase towards the galactic center

subhalo luminosity

$$L \propto \rho_s^2 r_s^3 \propto V_{\max}^4 / r_{V\max} \propto V_{\max}^3 \sqrt{c_V}$$

is practically unbiased,
i.e. proportional to DM density

galaxy halo boost factor

halo boost factor: $B = \dfrac{\text{total halo luminosity}}{\text{spherical, smooth halo luminosity}}$

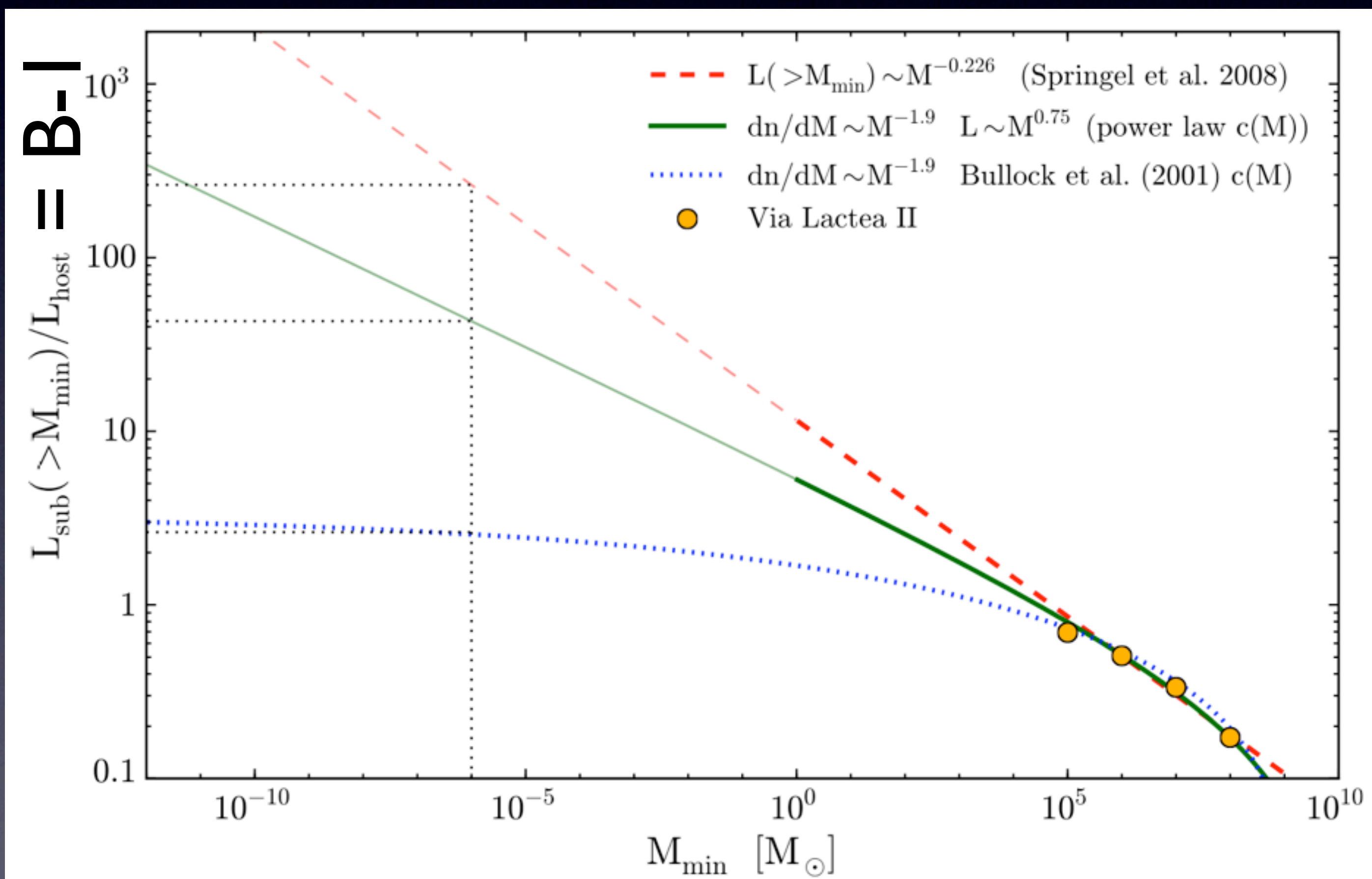

from Kuhlen et al. PDU, 2012

B ~ 4 - 15
JD et al ApJ 2006 and Nature 2008

maybe as high as B ~ 30
Kamionkowski et al. PRD 2010

not ~1.7
Stoehr, White, Springel et al. 2003

certainly not 232
Springel et al. Nature, 2008

certainly not 100 to 5000
Gao, Frenk et al. 2012

galaxy halo boost factor

$L_{sub}(>M_{min})$ and c(M) are not simple power laws,

CDM power spectrum ⟶ mass fluctuations ⟶ formation times

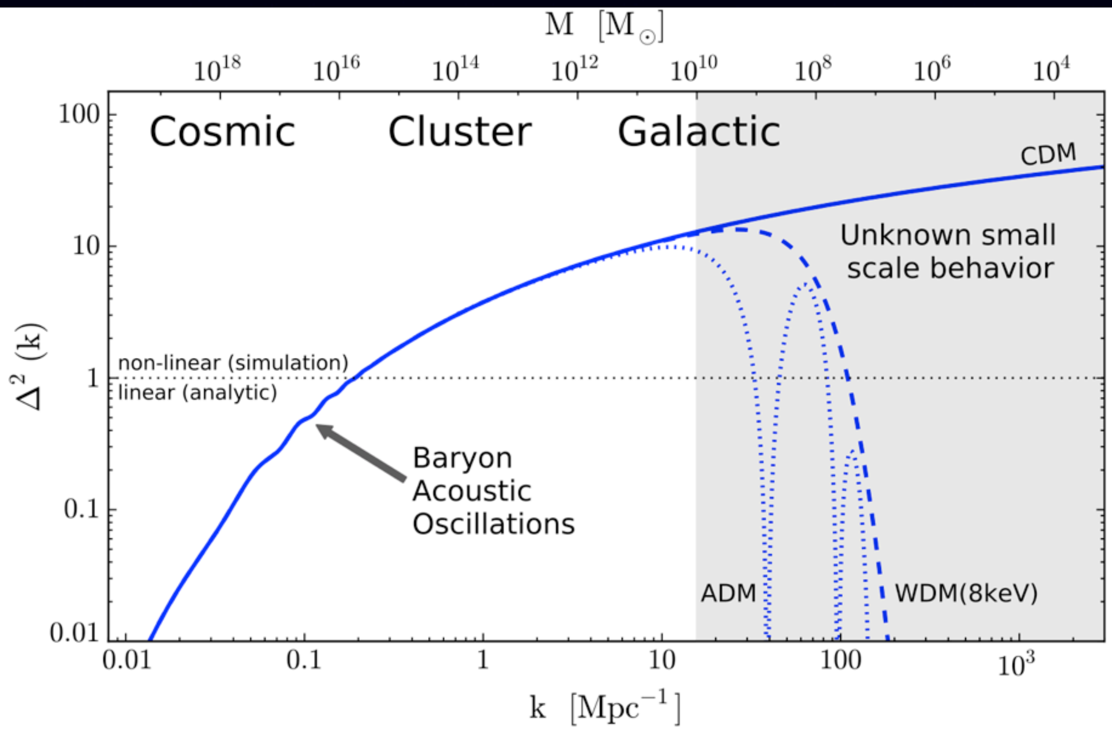

from Kuhlen et al. 2012

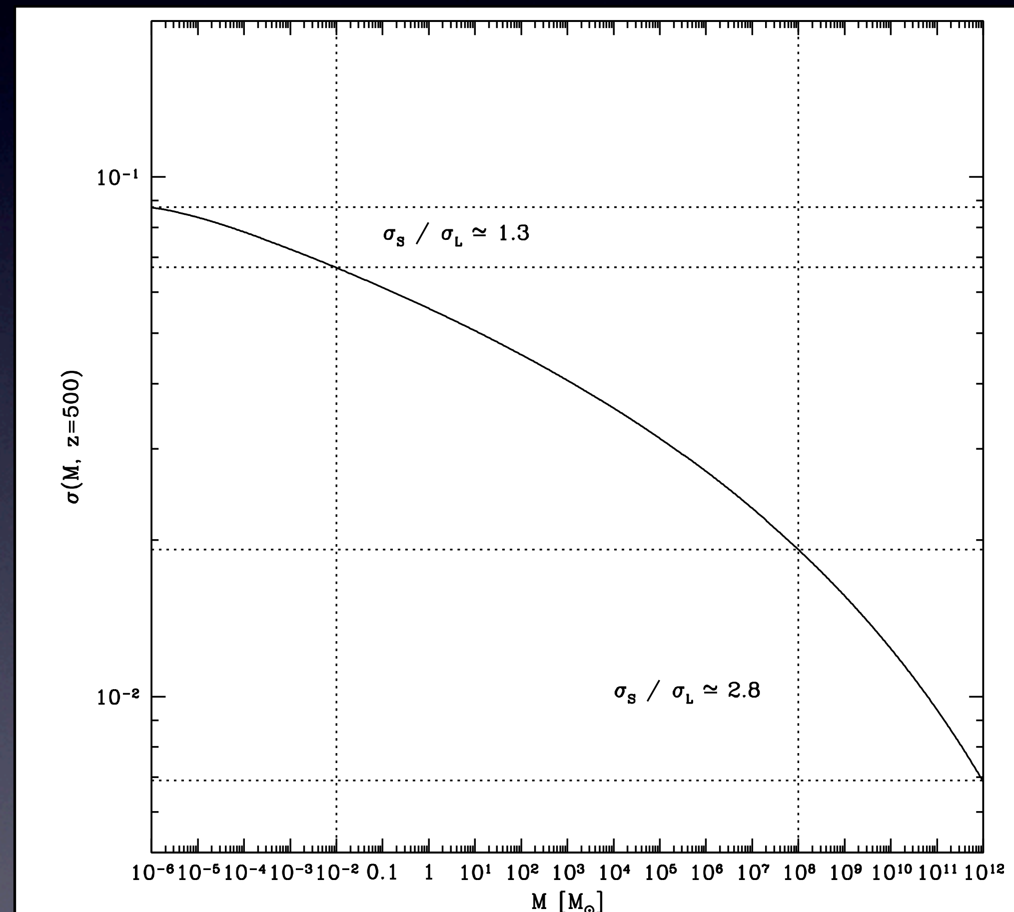

because p(k), sigma(M) and a_{form}(M) are not power laws.

boost factors

extrapolations to smallest
CDM subhalos depends on
the concentration - mass relation
Bullock et al. 2001 fits simulations well

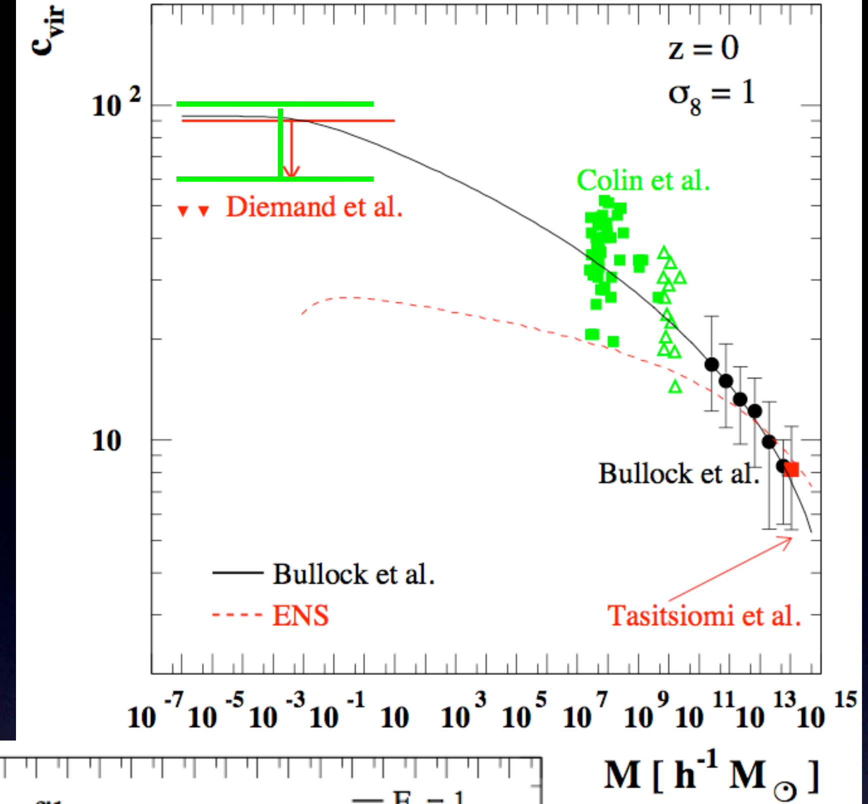

subhalos in mass decade
around one solar mass
contribute most to
total boost

moderate boost: B ~ 10
weak dependence on cutoff

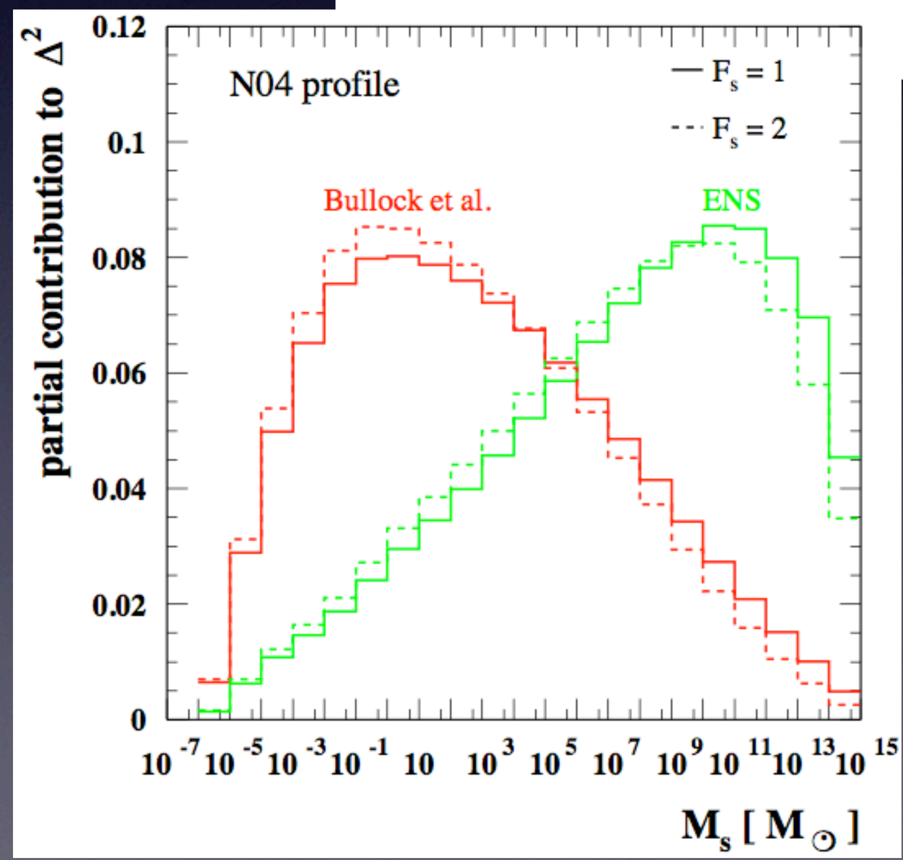

adapted from
Colafrancesco, Profumo, Ullio AA 2006

Colafrancesco, Profumo, Ullio AA 2006
JD et al. 2006/08
Kamionkowski, K PRD 2010
Anderhalden & JD, 2013; Sanchez-Conde+2013

boost factors depend on location

$$\text{halo boost factor} = \frac{\text{total halo luminosity}}{\text{spherical, smooth halo luminosity}}$$

~ 4 - 15   JD et al ApJ 2006 and Nature 2008

$$\text{local boost factor} = \frac{\text{total local luminosity}}{\text{smooth local halo luminosity}} \quad \sim 1.4 \pm 0.2$$

larger than 10 in only 1% of all locations at 8 kpc
too low to explain HEAT/PAMELA e+ excess with DM

JD et al, Nature 2008, Brun et al 2010

Allsky map of DM annihilation signal from via lactea II

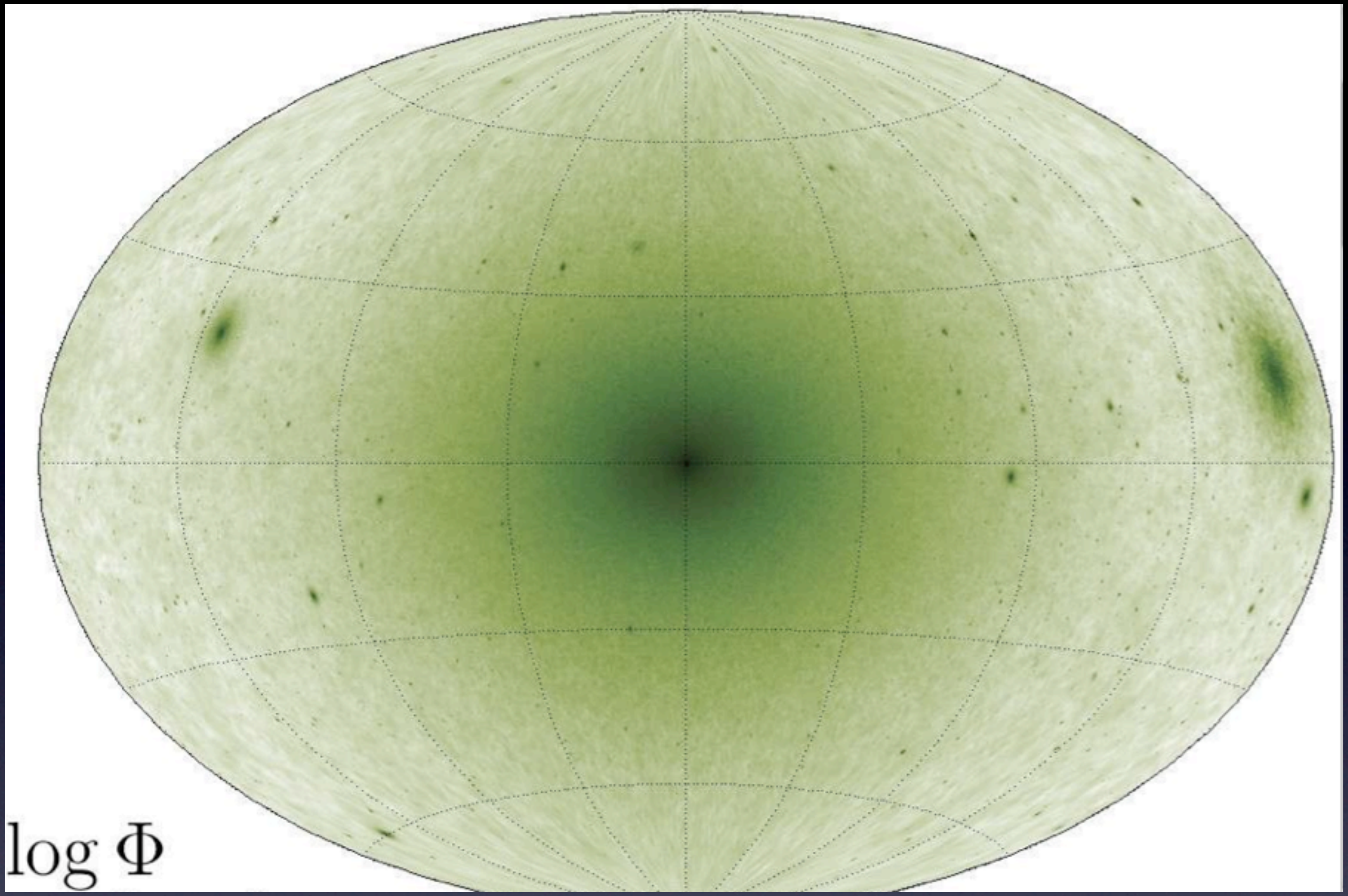

the main halo is obviously the brightest source

but due to poorly constrained, diffuse, astrophysical foregrounds
(e.g. Strong,Moskalenko,Riemer 2004),
subhalos are the more promising gamma ray sources (Baltz et al. 2008)

number of 3 and 5 sigma subhalo detection by GLAST/Fermi over 10 years

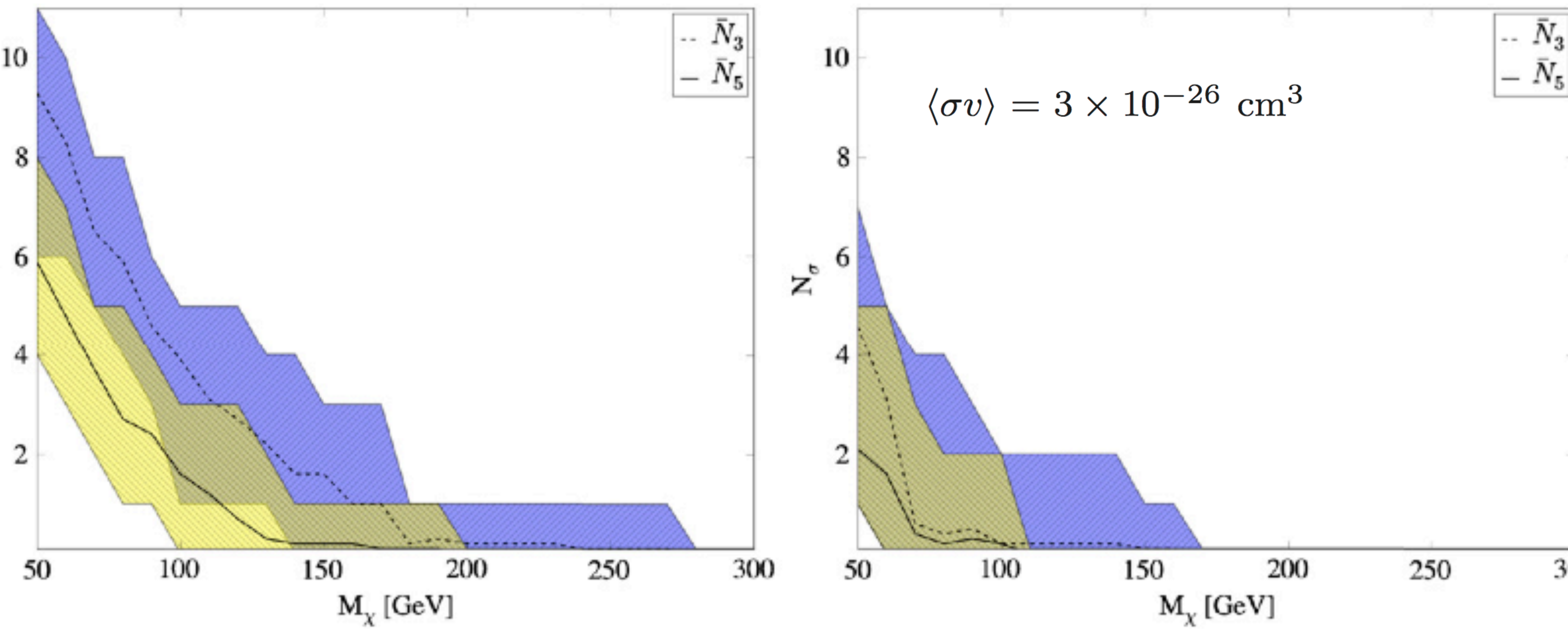

including unresolved small sub-subhalos

assuming no sub-subhalos

small scale sub-sub-structure is not crucial for detection, but it helps.

we find promising numbers for typical WIMP properties

Anderson, Kuhlen, JD, Johnson, Madau, ApJ 2011

4-year data from Fermi now starts to ru le out these models Ackermann+1310.0828

3. microhalos revisited

smallest scale CDM structures

For a 100 GeV SUSY neutralino (a WIMP) there is a cutoff at about 10^{-6} Msun due to free streaming

from Green, Hoffmann & Schwarz 2003

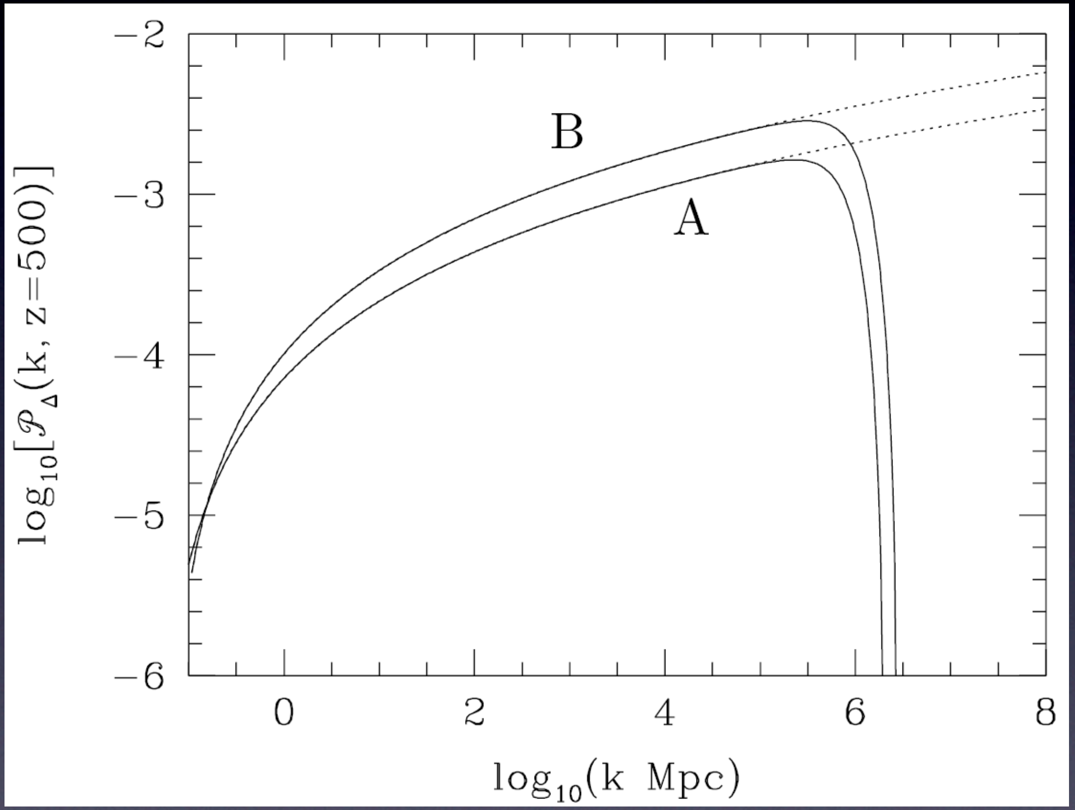

- small, “micro”-halos should forming around z=40 are the first and smallest CDM structures

smallest scale CDM structures

CDM microhalos seem to be about as cuspy as the larger halos that formed in mergers

their concentrations c ~ 3.3 at z=26
evolve into c ~ 90 by z=0
consistent with Bullock etal model

-> they are stable against tides caused by the MW potential if the live more than about 3 kpc form the galactic center

i.e. a huge number ~ 5×10^{15} could be orbiting in the MW halo today

(JD, Moore,Stadel, Nature 2005)

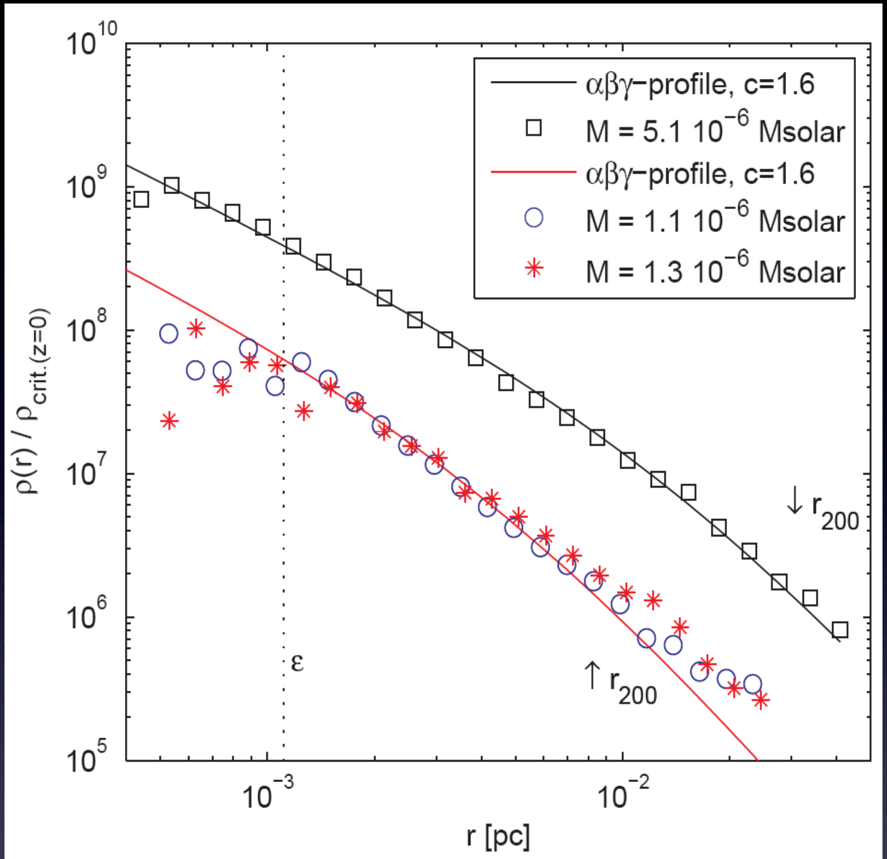

some tidal mass loss and disruption due to encounters with stars (see Goerdt+ astro-ph/0608495)

microhalo profiles depend on power spectrum

surprising result from Ishiyama et. al, ApJL, 2010:
cutoff leads to steeper profiles!

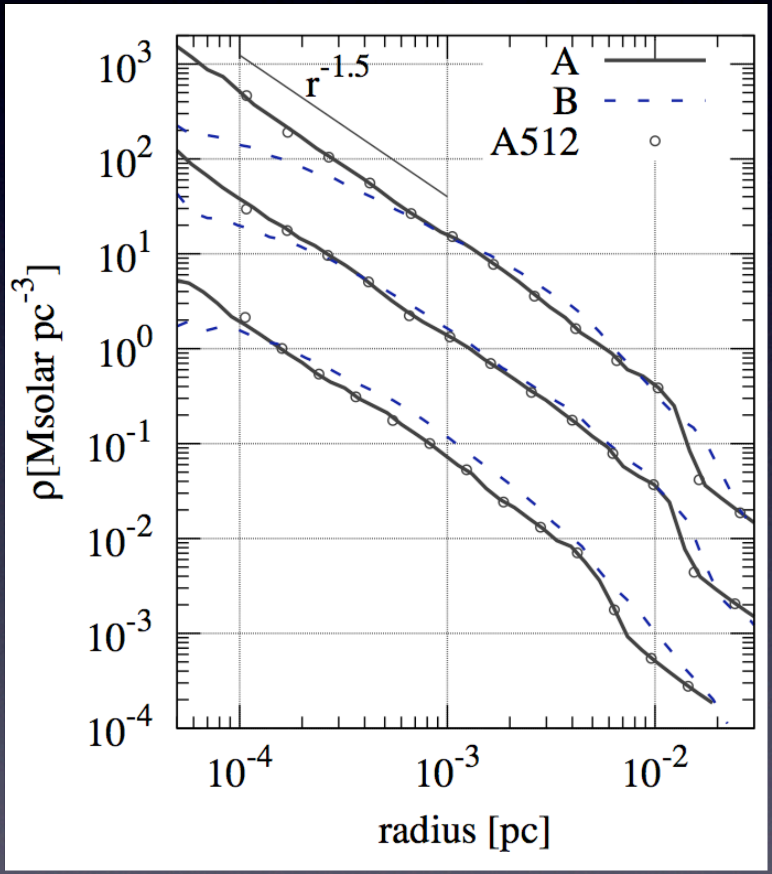

Ishiyama+, ApJL, 2010

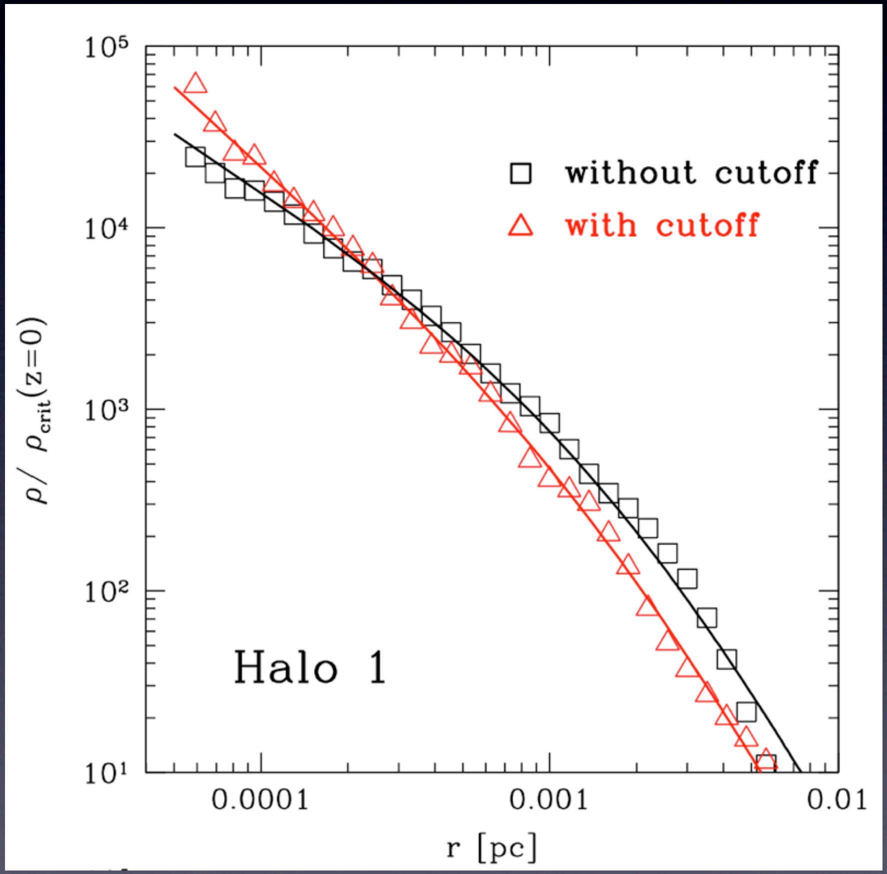

Anderhalden & JD, JCAP, 2013

microhalo profiles depend on power spectrum

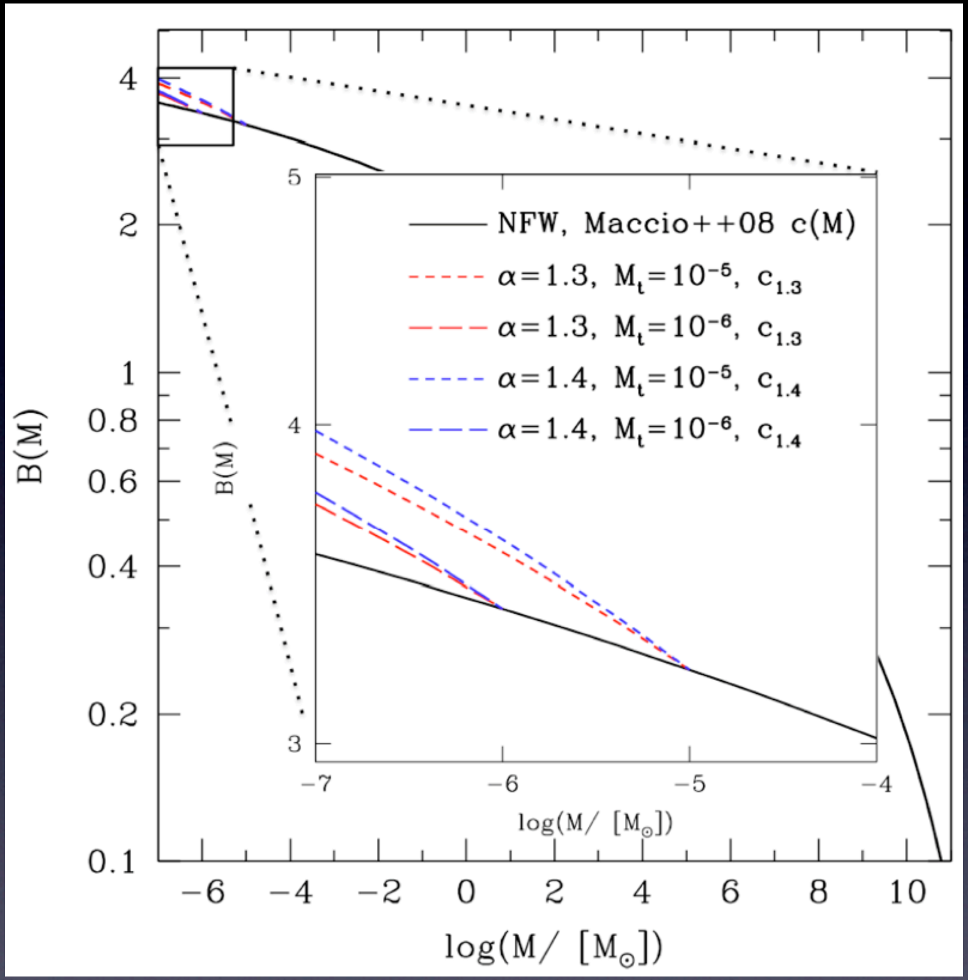

Anderhalden & JD, JCAP 2013

new, steeper microhalo profiles lead to larger boost factors

the effect is quite small: in this model the galactic halo boost increases from 3.5 to up to 4.0

high redshift microhalos show clear infall caustics

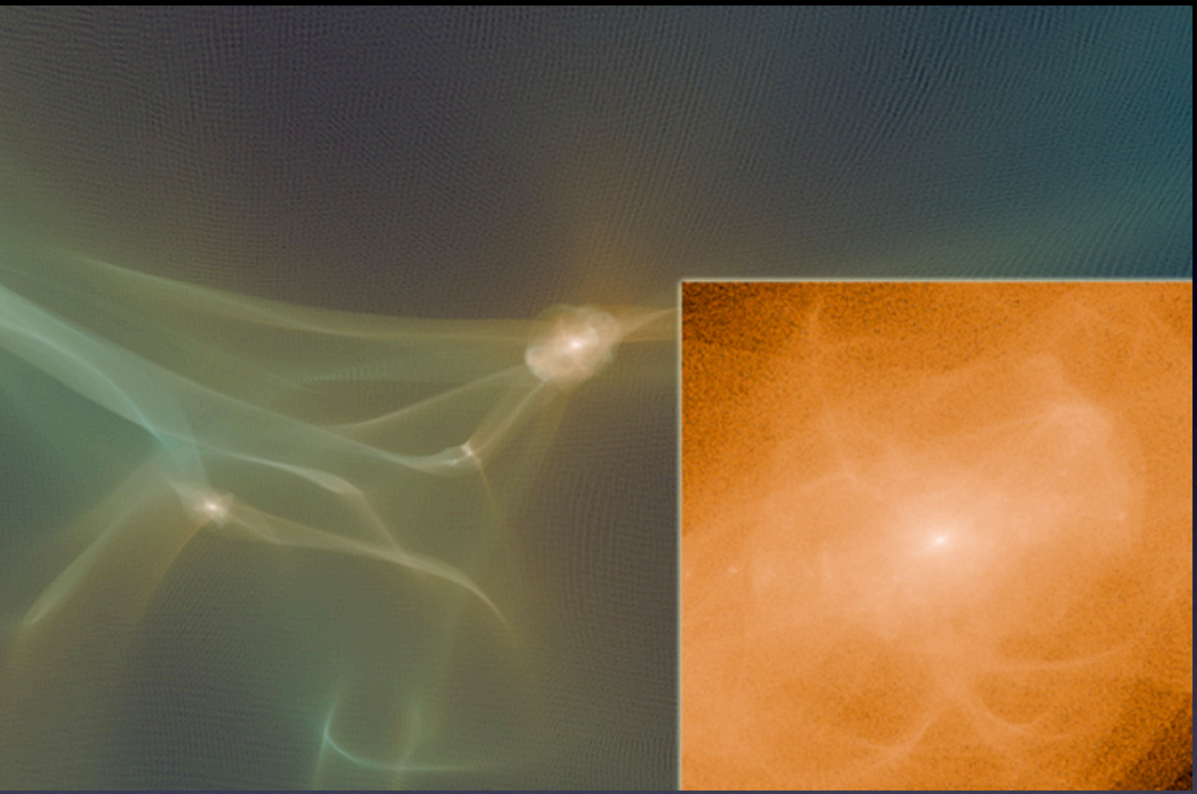

Ishiyama+, ApJL, 2010

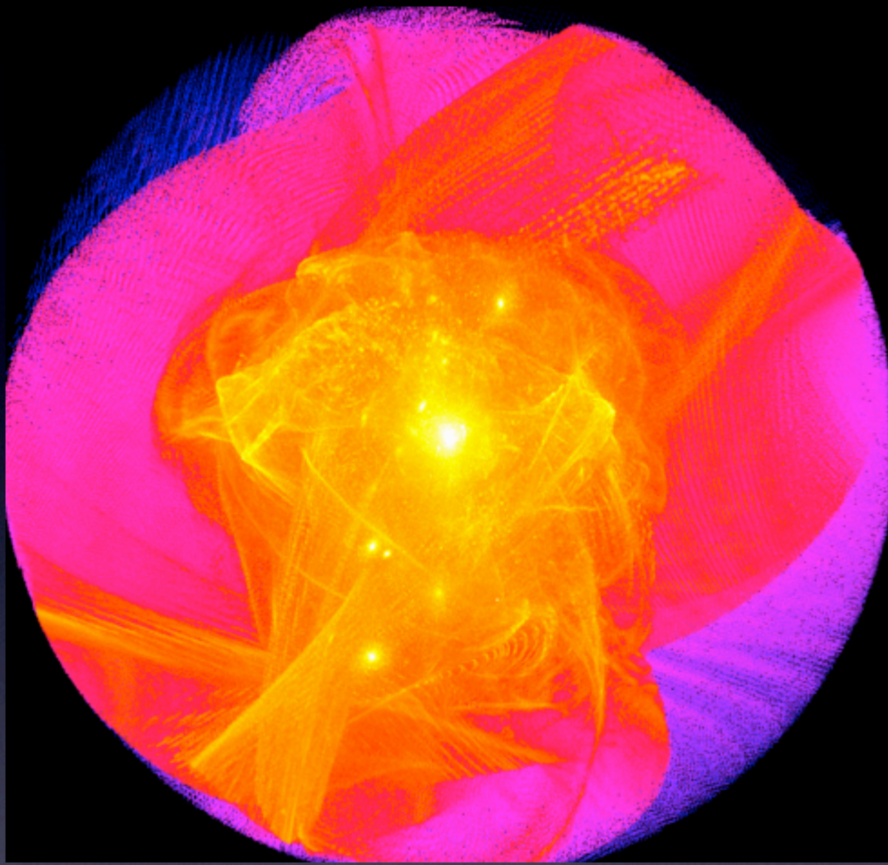

Anderhalden & JD, JCAP 2013

resolved caustics at z=30 increase the halo annihilation signal by 50%.
the effect decreases with time, unclear how much would be left at z=0.

summary of part A) N-body simulations of galactic dark matter

• identical density profiles and substructure abundance in the inner regions of field halos and subhalos, because tidal stripping affects mostly outer parts

• small halos and subhalos contribute significantly to the total DM annihilation signal. Largest contributions per mass decade come form around solar mass scales.

• astrophysical factors in pure CDM annihilation rates are now well constrained (within a factor of two). baryons increase the uncertainty in some regions

• subhalo annihilation signals might be detectable by GLAST/Fermi

• other substructures like infall caustics and tidal streams have little effect on direct and indirect DM detection

• microhalos near the cutoff have surprisingly steep inner profiles. this increases galactic halo boost factors by a small amount (up to 15 percent)

B) Molecular dynamics simulations of phase transitions

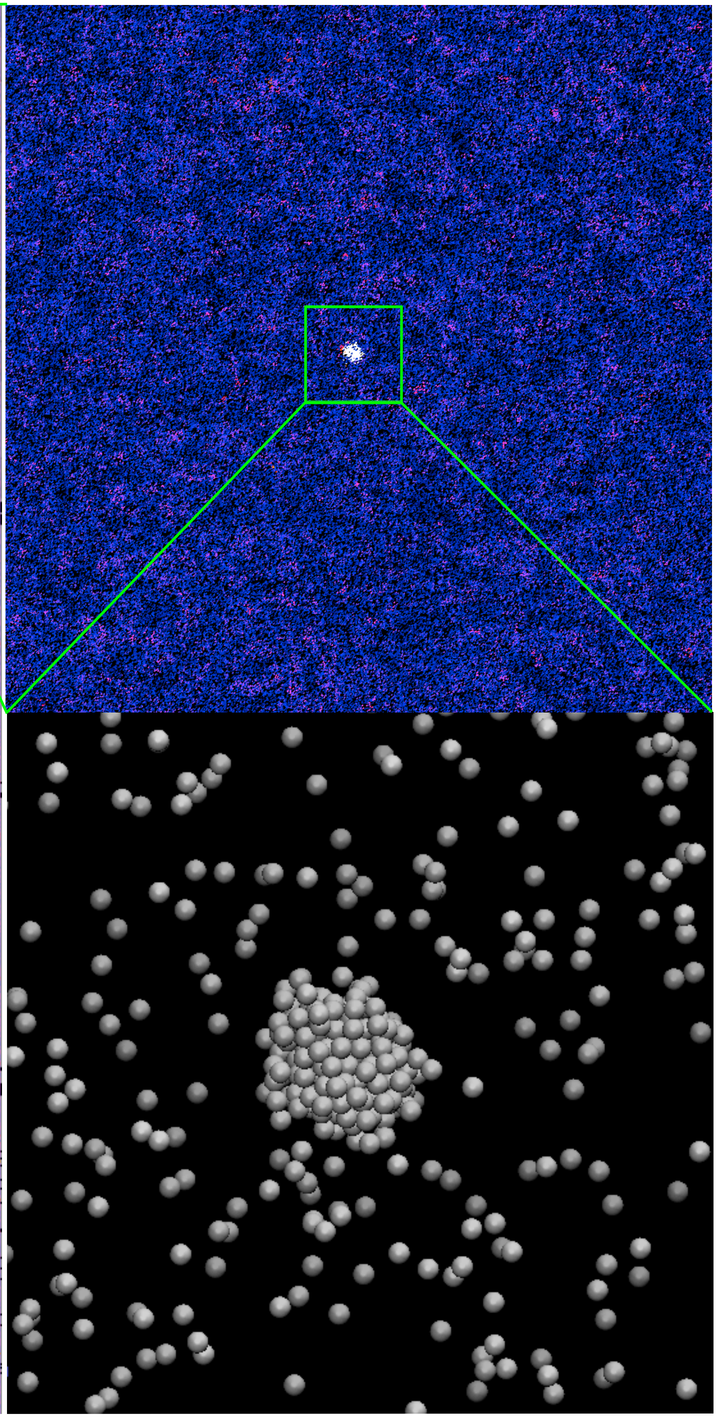

Jürg Diemand, University of Zurich

Raymond Angélil (U Zurich)
Kyoko K. Tanaka and Hidekazu Tanaka (Hokkaido U)

for details see:
Tanaka et al. J Chem Phys, 2005 and 2011
Diemand et al. J Chem Phys, 2013

Introduction to Homogeneous Nucleation

Phase transitions are important in many areas of science and technology, but we still lack accurate theoretical models.

In supersaturated vapor, the chemical energy is higher than the one of bulk liquid.

Forming the surface of the new phase comes at a cost.

Combining the positive surface term with the negative bulk term give rise to a maximum at a critical size N*.

Supersaturated vapor is a metastable state, for the transition to liquid the nucleation barrier ΔG(N*) has to be overcome.

The classical model assumes bulk liquid properties to describe the free energy of nano-clusters:

$$\frac{\Delta G_{i,\mathrm{CNT}}}{kT} = -i \ln S + \eta i^{2/3}$$

but its predictions differ from experiments and simulations by many orders of magnitudes.

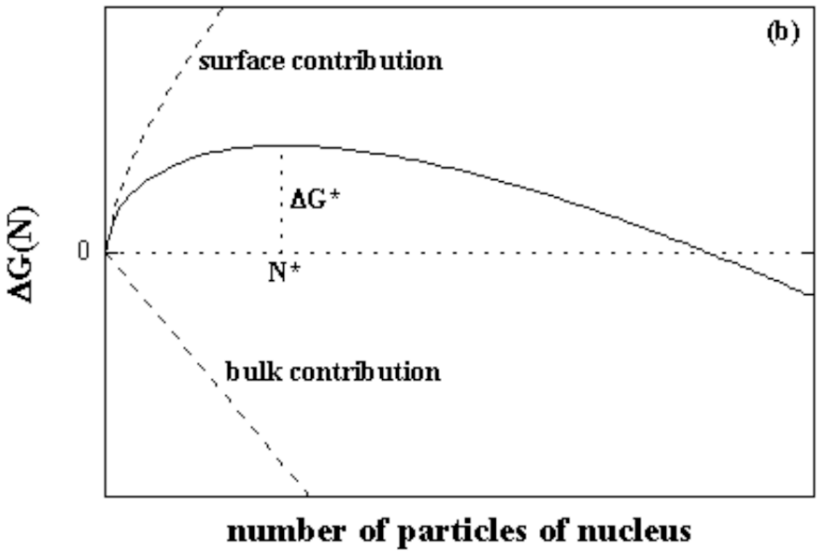

Yamada, PhD Thesis, 2003

direct molecular dynamics simulations of homogenous nucleation allow to resolve the process directly and to test theoretical models

Why large scale simulations?

- small simulations are limited to very high nucleation rates

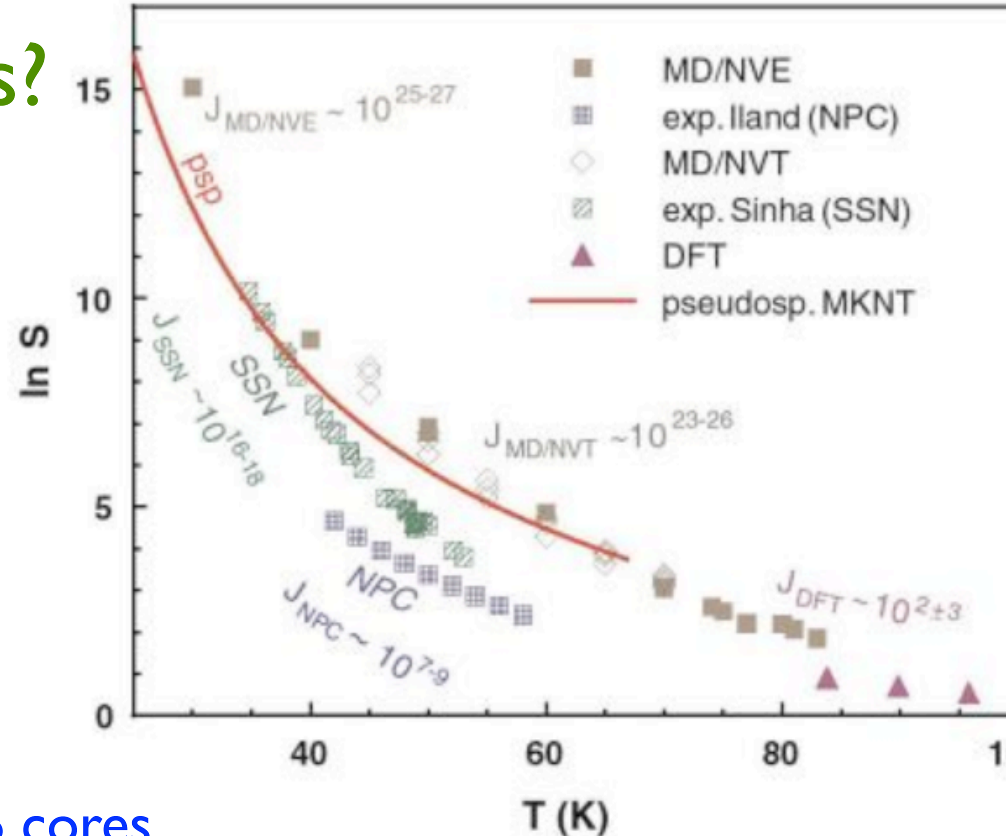

Kalikmanov, Nucleation Theory, Springer 2013

1 billion on 256 cores

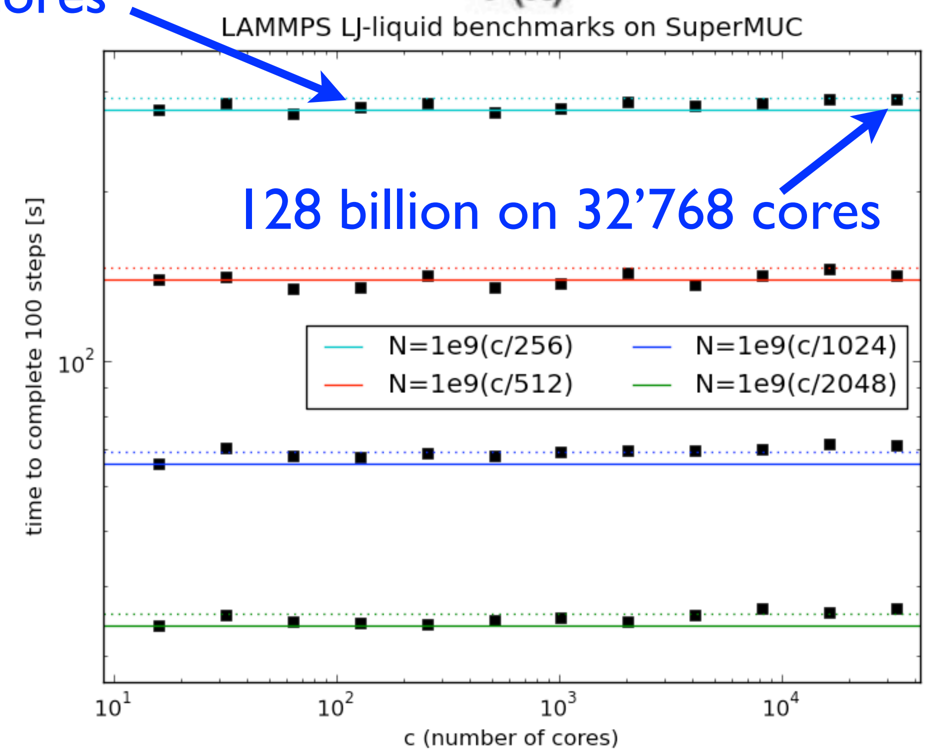

- lower nucleation rates can be resolved with longer runs, or with larger volumes. Large volumes (≡ many molecules) allow efficient usage of big supercomputers

Why large scale simulations?

- large volume simulations allow us to form a large number of clusters in a realistic, constant pressure vapor
- accurate nucleation rates
- less intervention required to keep the mean temperature constant
- good statistics on cluster properties

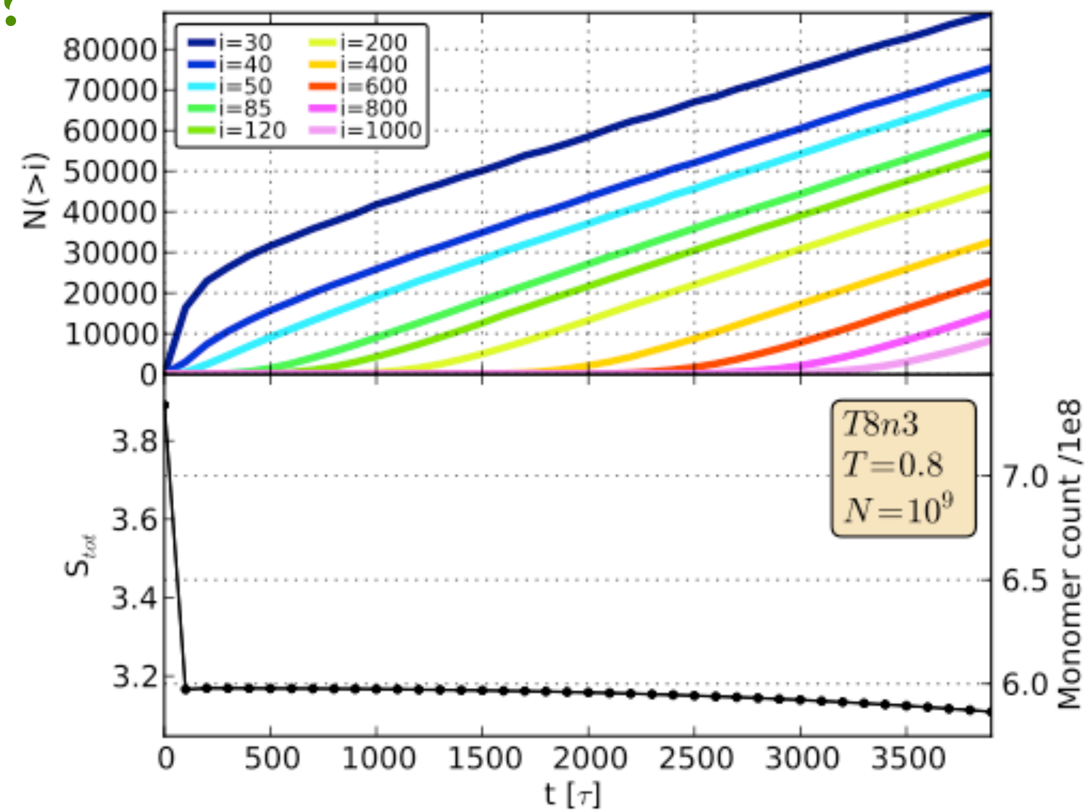

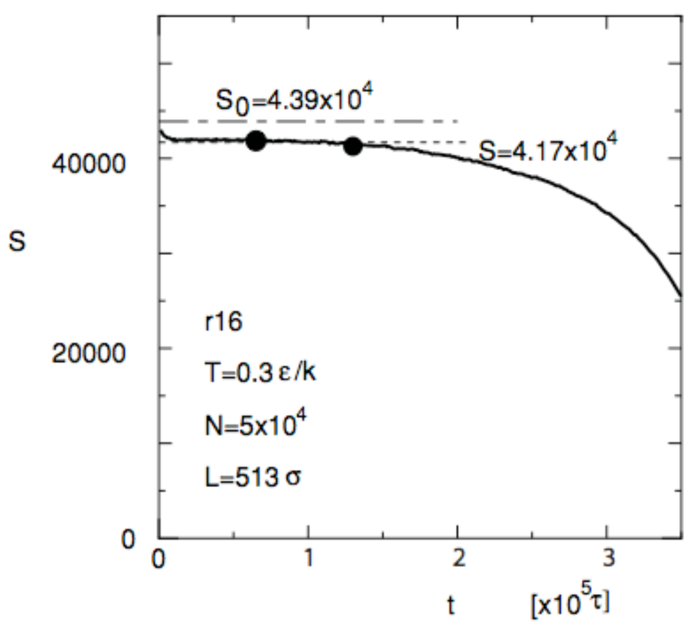

previous, smaller simulations had more evolution in S and produced few stable clusters

(from Tanaka et al. JCP, 2011)

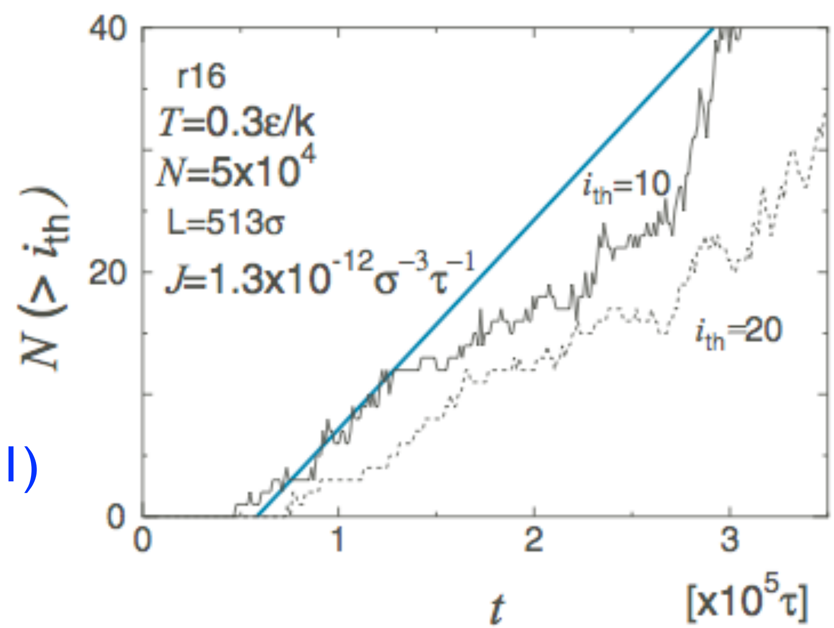

Simulation details

- LAMMPS, classical molecular dynamics code (Plimton 1995). Developed, maintained and distributed (open source) at Sandia National Lab.
- one to eight billion particles in a cube with periodic boundaries
- Lennard-Jones potential, cut-off and shifted to zero at 5σ
- constant, uniform time-step of standard size $0.01\ \tau = 0.0216$ ps
- random initial positions and velocities (speed limit avoids problems with initial overlap)
- mean temperature is kept constant with simple velocity rescaling
- 16 simulations over a wide range of temperatures (0.3 to 1.0 ε/k) and supersaturations
- liquid-like clusters are identified using the simple Stillinger-distance criterion with linking lengths of $r_c(T) = 1.60\sigma$, ... , 1.26σ

Computational resources

- PRACE award of 35 million core hours on HERMIT at HLRS, Germany

- CRAY XE6
  113 664 cores
  1.045 PFlops peak
  installed in 2011

- typical run:
  one billion atoms
  16’384 cores
  ~ 100k steps/hour

Nucleation rates from MD

- we use the Yasuoka-Matsumoto method (threshold method):

$$J = \frac{1}{V}\frac{dN(>i)}{dt}$$

- most of our runs allow a very accurate determination of J. results are independen of t and i (after some lag time)
- some runs with the very low rates only allow for rough estimates or upper limits

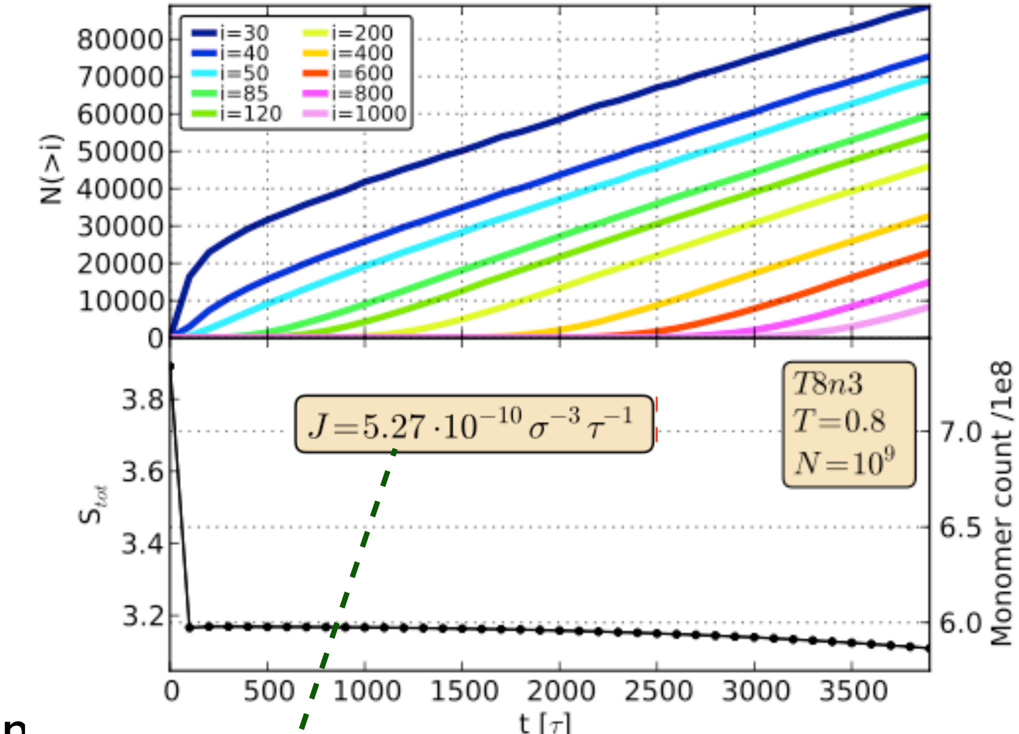

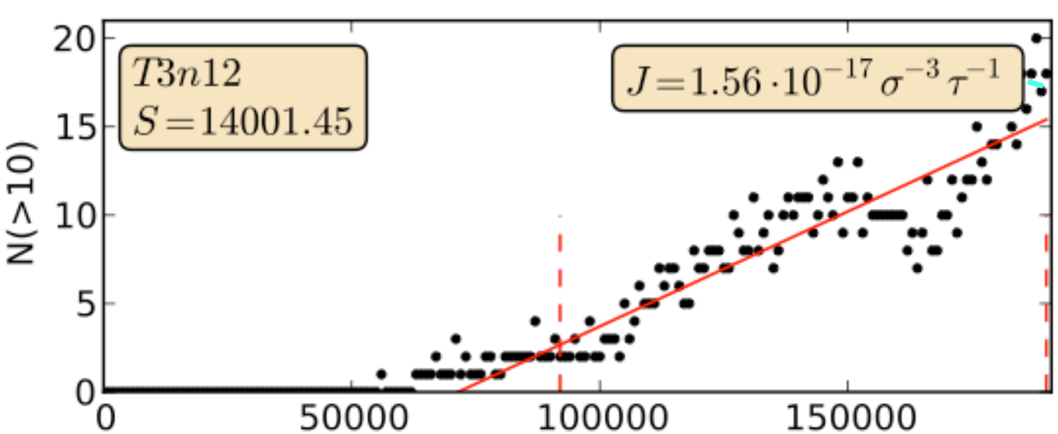

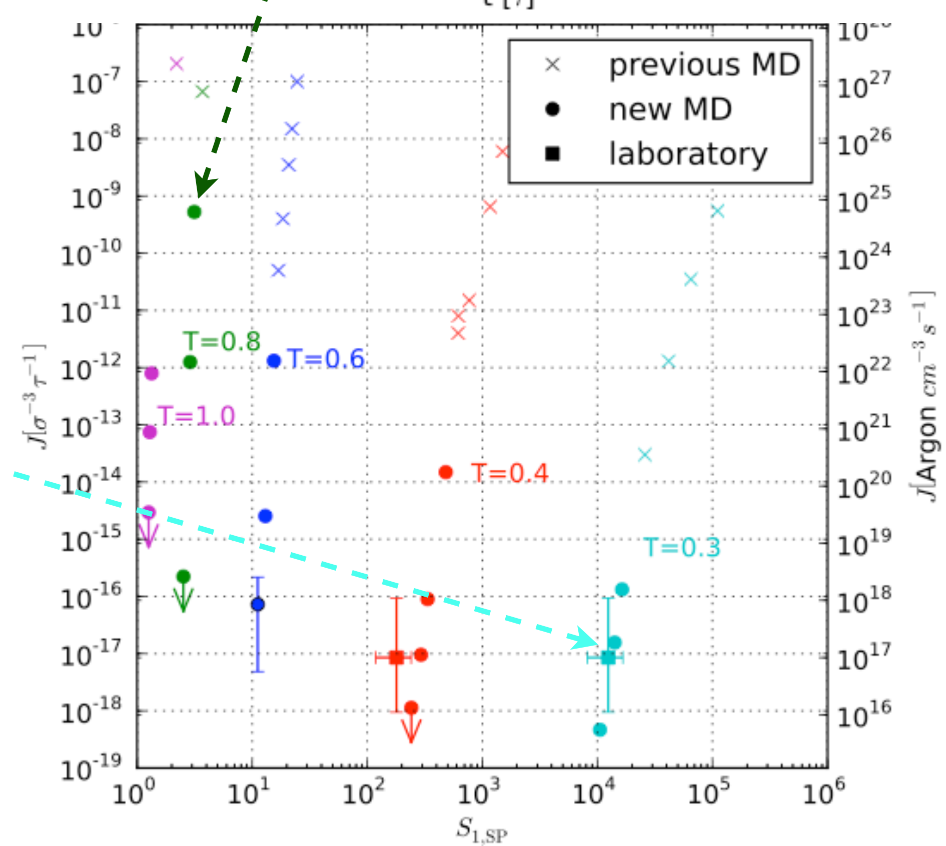

Diemand et al. JCP submitted 2013

Nucleation rates: MD vs SSN experiment

- assuming the standard Argon system, ε/k = 119.8 K, σ = 3.405 Å, we find good agreement with the Supersonic Nozzle (SSN) experiment (Sinha et al. 2010)

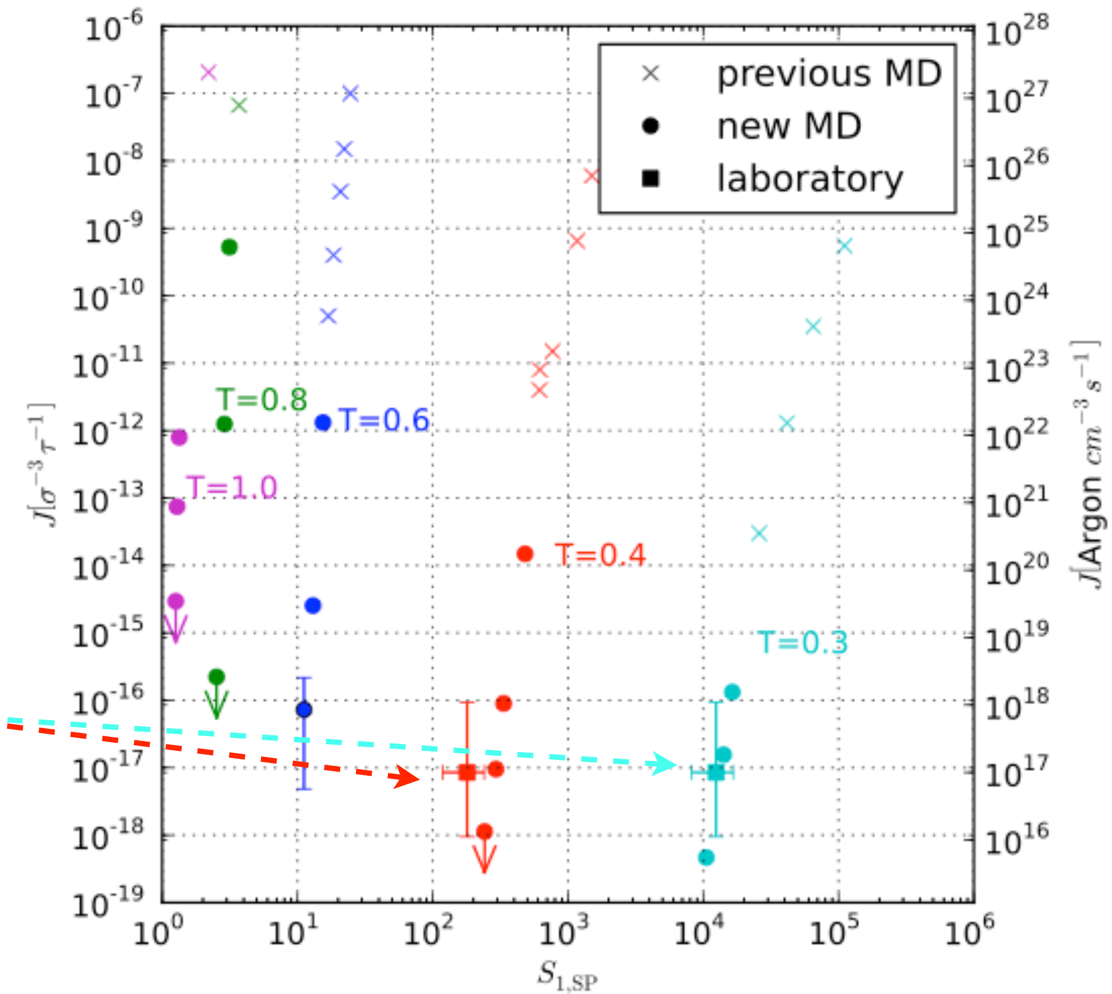

Nucleation rates: MD vs CNT and SP model

in classical models the nucleation rate is

$$J = \left[\sum_{i=1}^{\infty} \frac{1}{R^+(i) n_e(i)}\right]^{-1} \simeq R^+(i^*) n_e(i^*) Z$$

with transition rates $R^+(i)$

$$R^+(i) = \frac{di}{dt} = \alpha n_e(1) \nu_{\text{th}}\, 4\pi r_0^2 i^{2/3}$$

(evaporation is neglected and α is set to one)
the equilibrium abundances $n_e(i)$ are

$$n_e(i) = \frac{P_1}{kT} \exp\left[-\frac{\Delta G_i}{kT}\right]$$

the free energies ΔG_i are given by the models

$$\frac{\Delta G_{i,\text{CNT}}}{kT} = -i \ln S + \eta i^{2/3},$$
$$\frac{\Delta G_{i,\text{MCNT}}}{kT} = -(i-1) \ln S + \eta(i^{2/3} - 1), \quad \text{and}$$
$$\frac{\Delta G_{i,\text{SP}}}{kT} = -(i-1) \ln S + \eta(i^{2/3} - 1) + \xi(i^{1/3} - 1)$$

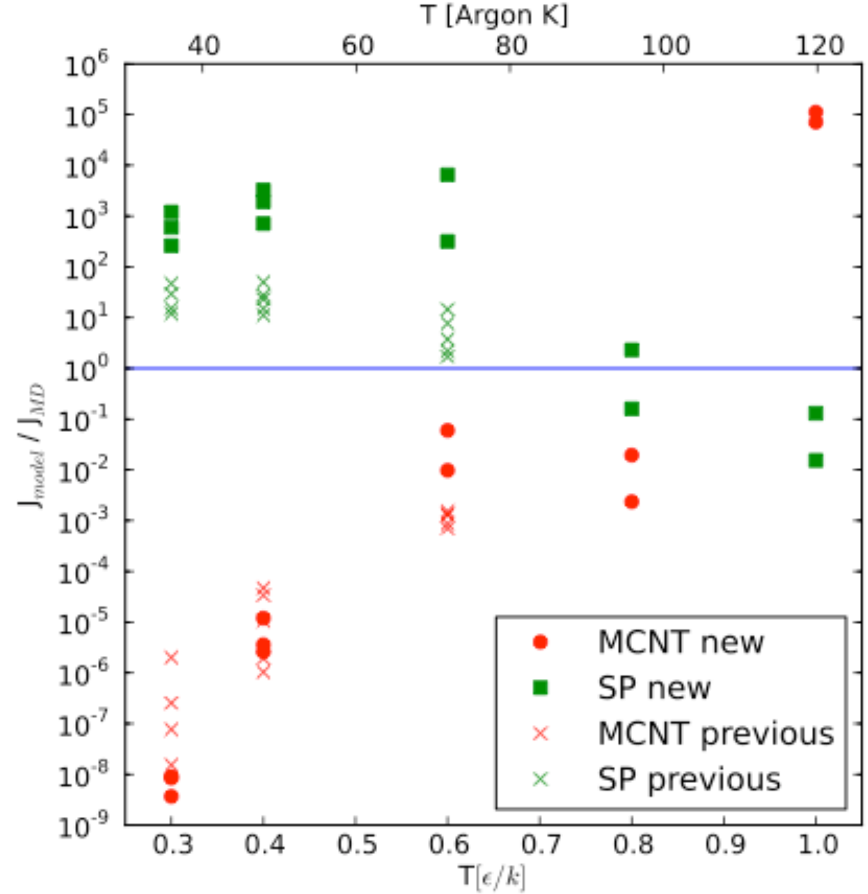

rates from CNT and MCNT (Modified/ self-consistent CNT) have a very different temperature dependence

the semi-phenomenological (SP) model (Dillmann&Meier,1991) matches previous, high-J MD simulations well, but differs from our new results by up to 10^4

Summary of part B) Molecular dynamics simulations of phase transitions

- large scale MD simulations of homogenous nucleation allow us to resolve far lower nucleation rates than previous MD simulations

- direct comparisons with laboratory experiments are now possible. we find perfect agreement with SSN Argon experiments at 36 K, although the temperature dependence appears to be different

- our simulations confirm that classical models (CNT and MCNT) fail by large factors at most temperatures

- the Dillmann-Meier semi-phenomenological model matches results from earlier, high-J simulations well, but differs from our lowest-J runs by up to 10^4